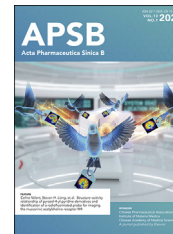




Chinese Pharmaceutical Association
Institute of Materia Medica, Chinese Academy of Medical Sciences

Acta Pharmaceutica Sinica B

www.elsevier.com/locate/apsb
www.sciencedirect.com



ORIGINAL ARTICLE

Bile duct ligation differently regulates protein expressions of organic cation transporters in intestine, liver and kidney of rats through activation of farnesoid X receptor by cholate and bilirubin



Shijin Hong^a, Shuai Li^a, Xiaoyan Meng^b, Ping Li^a, Xun Wang^a,
Mengxiang Su^c, Xiaodong Liu^{a,*}, Li Liu^{a,*}

^aCenter of Drug Metabolism and Pharmacokinetics, School of Pharmacy, China Pharmaceutical University, Nanjing 210098, China

^bTianjin Institutes of Pharmaceutical Research, Tianjin 300301, China

^cDepartments of Pharmaceutical Analysis, School of Pharmacy, China Pharmaceutical University, Nanjing 210098, China

Received 1 April 2022; received in revised form 17 May 2022; accepted 1 June 2022

KEY WORDS

Bilirubin;
Chenodeoxycholic acid;
Farnesoid X receptor;
Liver failure;
Organic cation transporters;
Bile duct ligation;
Physiologically based pharmacokinetic model

Abstract Body is equipped with organic cation transporters (OCTs). These OCTs mediate drug transport and are also involved in some disease process. We aimed to investigate whether liver failure alters intestinal, hepatic and renal Oct expressions using bile duct ligation (BDL) rats. Pharmacokinetic analysis demonstrates that BDL decreases plasma metformin exposure, associated with decreased intestinal absorption and increased urinary excretion. Western blot shows that BDL significantly downregulates intestinal Oct2 and hepatic Oct1 but upregulates renal and hepatic Oct2. *In vitro* cell experiments show that chenodeoxycholic acid (CDCA), bilirubin and farnesoid X receptor (FXR) agonist GW4064 increase OCT2/Oct2 but decrease OCT1/Oct1, which are remarkably attenuated by glycine- β -muricholic acid and silencing FXR. Significantly lowered intestinal CDCA and increased plasma bilirubin levels contribute to different Oct regulation by BDL, which are confirmed using CDCA-treated and bilirubin-treated rats. A disease-based physiologically based pharmacokinetic model characterizing intestinal, hepatic and renal Oct was successfully developed to predict metformin pharmacokinetics in rats. In conclusion, BDL remarkably downregulates expressions of intestinal Oct2 and hepatic Oct1 protein while

*Corresponding author. Tel./fax: +86 25 83271060.

E-mail addresses: xdliu@cpu.edu.cn (Xiaodong Liu), liulee@cpu.edu.cn (Li Liu).

Peer review under responsibility of Chinese Pharmaceutical Association and Institute of Materia Medica, Chinese Academy of Medical Sciences.

upregulates expressions of renal and hepatic Oct2 protein in rats, finally, decreasing plasma exposure and impairing hypoglycemic effects of metformin. BDL differently regulates Oct expressions *via* Fxr activation by CDCA and bilirubin.

© 2023 Chinese Pharmaceutical Association and Institute of Materia Medica, Chinese Academy of Medical Sciences. Production and hosting by Elsevier B.V. This is an open access article under the CC BY-NC-ND license (<http://creativecommons.org/licenses/by-nc-nd/4.0/>).

1. Introduction

The body is equipped with polyspecific organic cation transporters (OCTs), accounting for uptake, distribution and elimination of endogenous organic cations, cationic drugs and toxins¹. OCT1–3, characterizing extensively overlapping substrate specificities, mediates transport of some cationic drugs such as cephaloridine, metformin and cimetidine. OCTs also transport some endogenous cationic substances including choline, thiamine, creatinine, serotonin, dopamine and norepinephrine. OCT2/SLC22A2 is mainly expressed at basolateral membrane of renal tubules, while OCT1/SLC22A1 is mainly expressed on the sinusoidal membrane of hepatocytes^{2,3}. Small intestine also expresses OCT1, OCT2 and OCT3/SLC22A3^{2,3}. OCTs expressed in intestine, liver and kidney, along with multidrug/toxin extrusions (MATE1/2), commonly control intestinal absorption, hepatic uptake, biliary excretion and renal secretion of organic cation compounds, constructing interplay of intestine, liver and kidney. Moreover, OCTs are also involved in some disease process. A mouse experiment shows that Oct3 deletion enhances liver fibrosis by thioacetamide (TAA) and bile duct ligation (BDL)⁴. Feeding with a high-fat diet increases gentamicin-induced nephrotoxicity due to higher accumulation of gentamicin by induction of renal Oct2 expressions⁵. On the contrast, Oct1/2 double-knockout protects from ototoxicity and partly from nephrotoxicity by cisplatin in mice⁶. The downregulation of OCT1 is associated with tumor progression of cholangiocellular carcinoma and worse overall patient survival rates⁷. Metformin is actively transported into the liver by OCT1. Clinic trials have demonstrated that reduced-function variants in SLC22A1 attenuate the ability of metformin to reduce both glucose excursion in response to oral glucose⁸ and level of the blood glycosylated hemoglobin in patients with type 2 diabetes⁹.

Thiamine, an important water-soluble vitamin, plays a central role in various biological processes. Our bodies cannot synthesize thiamine and thiamine needs to be ingested from food¹⁰. Intestinal absorption and renal excretion of thiamine are mainly mediated by identified transporters. The identified transporters related to thiamine transport include thiamine transporter 1 (THTR1), THTR2, OCTs and MATEs^{2,11}. THTR1 and THTR2 are also expressed in intestine, hepatocytes and kidney. Contribution of THTR2 to intestinal absorption of thiamine is more important than THTR1¹² and THTR2 is required for intestinal uptake of thiamine¹². Moreover, THTR2 also mediates intestinal absorption of metformin¹³.

Liver failure is often associated with thiamine deficiency¹⁴. A clinical report has showed that 18 out of 31 patients with chronic liver disease characterize thiamine deficiency¹⁵. Labadarios et al.¹⁶ reported that 9 out of 24 patients with fulminant liver failure are associated with thiamine deficiency. Blood thiamine levels in patients with acute liver failure^{17,18} and acute-on-chronic liver failure¹⁸ are significantly lower than those in healthy subjects. Liver failure also alters expressions of transporters, in turn,

affecting pharmacokinetics and efficacy of some drugs^{19–24}. Our pre-experiment also shows that liver failure by BDL downregulates expressions of intestinal Oct2 protein but upregulates expressions of renal Oct2 protein without affecting expressions of intestinal Thtr2 and renal Mate1 protein, indicating that thiamine deficiency by liver failure may be attributed to downregulation of intestinal Oct2 expressions or upregulation of renal Oct2 expressions, which needs investigation.

Significant increases in bilirubin and bile acids are observed in the serum of patients with liver failure and liver failure animals^{21–23,25}. Our pre-experiment also shows that BDL significantly reduces the concentration of intestinal bile acids and increases levels of bilirubin in serum of rats, which may become factors that BDL differently regulates expressions of Octs in intestine, liver and kidney of rats.

The aims of the study were: 1) to investigate different alterations in expressions and function of Octs in liver, intestine and kidney of BDL-induced liver failure rats; 2) to investigate whether increases in levels of serum bilirubin and decreases in levels of intestinal bile acid become reasons that BDL differently regulates function and expressions of Octs in liver, intestine and kidney of rats using Caco-2 cells, human kidney-2 (HK-2) cells and HepG 2 cells as *in vitro* models, which were further confirmed using rats treated with chenodeoxycholic acid (CDCA) and bilirubin; 3) to establish a disease-based physiological pharmacokinetic (PBPK) model for analyzing individual contribution of alterations in expressions and functions of intestinal, hepatic and renal Octs to the pharmacokinetic behaviors of metformin, a typical Oct substrate, in BDL rats and their integrated effects. The results would highlight the clinical significance of alterations in the expressions and function of intestinal, hepatic and renal Octs under liver failure.

2. Materials and methods

2.1. Materials

All materials used in the study are commercially available and listed in [Supporting Information Table S1](#).

2.2. Animals

Male Sprague–Dawley rats, weighing 200–250 g, were obtained from Super-B&K Laboratory Animal Co. (Shanghai, China). Rats were kept in an air-conditioned (25 ± 2 °C) room with a controlled 12 h/12 h light-dark cycle and relative humidity (50 ± 5%). Rats were maintained on regular chow with drinking water available *ad libitum*. The animal studies were performed in accordance with the Guide for the Care and Use of Laboratory Animals (National Institutes of Health) and approved by the China Pharmaceutical University Animal Ethics Committee (No. 2020-03-003).

2.3. Development of BDL rats

BDL rats were developed according to a method previously described²³. Briefly, rats were anesthetized *via* intraperitoneal (ip) injection of pentobarbital (60 mg/kg). The common bile duct was exposed through a midline incision in the abdomen and triple-ligated with 4-0 silk suture. In sham-operated (Sham) animals, the common bile duct was exposed without ligation. The abdominal incision was closed. The rats were allowed to recover. On the 14th day following surgical operation, the BDL and Sham rats were used for the following experiments.

2.4. Pharmacokinetics of metformin after oral or intravenous administration to experimental rats

Metformin, a typical substrate of OCTs and MATEs, is absorbed through the small intestine and almost is excreted *via* the kidney as a prototype²⁶. Functions of intestinal Octs and renal Octs/Mates were assessed using alterations in pharmacokinetics of metformin. On the 14th day after surgical operation, pharmacokinetics of metformin in BDL and Sham rats following oral and intravenous administration were investigated. In brief, the experimental rats, fasted overnight, orally (40 mg/kg) or intravenously (10 mg/kg) received metformin (dissolved in normal saline). The dosage of metformin was designed based on previous reports^{27,28}. Blood samples (about 150 μ L) were collected into heparinized micro-centrifuge tubes at designated times (15, 30, 45, 60, 90, 120, 240 and 360 min for oral dose; 5, 10, 15, 30, 60, 90, 120, 240 and 360 min for intravenous dose) after administration *via* the oculi chorioideae vein under light ether anesthesia and plasma samples were obtained. After each 4 samplings, a suitable amount of normal saline was administered to the experimental rats *via* the tail vein to compensate for blood loss. Plasma concentrations of metformin were measured using HPLC method²⁸.

Oral glucose tolerance test (OGTT) was also performed. Briefly, both Sham and BDL rats were divided into metformin-treated rats and control rats. The rats, fasted overnight, at 30 min after orally receiving 150 mg/kg metformin or vehicle, were orally administrated glucose (2 g/kg). The blood glucose levels were measured by glucometer (Accuchek performa, Roche) at 0, 15, 30, 60 and 90 min post glucose dose *via* tail tip cut.

2.5. Expressions of Octs and Mates in intestine, liver and kidney of rats

On the 14th day after surgical operation, the rats, fasted overnight, were sacrificed under diethyl ether anesthesia. Blood samples were collected and serum samples were obtained for measuring serum biochemical parameters, respectively. Intestine, liver and kidney were quickly obtained for determining the expressions of targeted proteins and their mRNA. The intestinal contents were also collected by infusion of 5 mL 0.9% saline. Levels of bile acids in intestinal contents, plasma, liver and kidney were measured using LC-MS²⁹ (illustrated in supplement). Bilirubin levels in kidney and intestinal contents were detected using assay kits and blood thiamine concentrations were detected using HPLC-FLU method³⁰.

2.6. Intestinal absorption of metformin and thiamine in rat duodenum

Absorption of metformin and thiamine in the duodenum of rats was evaluated by *in situ* single-pass perfusion according to a

previous protocol³¹. Briefly, the experimental rats, fasted overnight, were anesthetized with pentobarbital (60 mg/kg, ip). The duodenum segment (about 10 cm) was isolated, and two cannulas were inserted at either end of the isolated duodenum. The isolated intestinal segment was perfused with Krebs-Hensley buffer (37 °C) for 10 min, followed by Krebs-Hensley buffer containing metformin (50 μ g/mL), metformin (50 μ g/mL) with dopamine (20 μ mol/L), metformin (50 μ g/mL) with estradiol (1 μ mol/L), metformin (50 μ g/mL) with corticosterone (4 μ mol/L), thiamine (20 μ g/mL) or thiamine with corticosterone (4 μ mol/L) at 0.2 mL/min for \sim 30 min. Then, consecutive effluent samples were collected every 15 min for 90 min *via* the distal cannula. The levels of metformin and thiamine in outflow were measured. The concentrations of metformin and thiamine were designed according to the preliminary data. At the end of perfusion, the rats were sacrificed, and the area of perfused intestinal segments A (cm^2) was measured. The apparent effective permeability (P_{eff} , cm/min) was estimated using Eq. (1):

$$P_{\text{eff}} = -Q \times \ln(C_{\text{out}}/C_{\text{in}})/A \quad (1)$$

where C_{in} and Q (mL/min) are the metformin or thiamine concentration in the inflow and the flow rate, respectively. C_{out} was the metformin or thiamine concentration at the outflow and was corrected by the weight calibration method.

2.7. Urinary secretion of thiamine and metformin in rats

Urinary secretions of thiamine and metformin in rats were measured. The experimental rats were housed in metabolic cage and the 6 h urinary samples of each rat were collected for measuring recovery of thiamine. Then, the experimental rats intravenously received dose (10 mg/kg) of metformin and recovery of metformin during 6 h was also measured.

Precision-cut kidney slices were documented to further investigate renal uptake of metformin. Prepare experimental rat kidney sections (about 300 μ mol/L) according to conventional techniques. After pre-incubation in oxygenated incubation medium (120 mmol/L NaCl, 16.2 mmol/L KCl, 10 mmol/L sodium phosphate, 1.2 mmol/L MgSO₄, 1.0 mmol/L CaCl₂ buffer, pH 7.4) at 37 °C for 5 min, the slices were transferred to a 24-well plate in 1 mL incubation medium containing metformin (50 μ g/mL) and incubated at 37 °C for 15 min. Following washing three times with ice-HBSS (pH 7.4), the slices were blotted using the filter paper and weighed. Amount of metformin (μ g/g slice) in the slices was measured.

2.8. In vivo tissue uptake of metformin by liver and kidney

The uptake clearance (CL_{uptake}) by the liver and kidney was determined within 3 min following iv administration of metformin according to previous report¹⁹. The experimental rats were anesthetized with pentobarbital (60 mg/kg, ip), the femoral artery and vein were cannulated with a polyethylene tube (PE-50), filled with heparinized saline (20 IU/mL). Metformin (10 mg/kg) was intravenously administrated to the experimental rats. Blood samples were collected at 0, 0.5, 1, 2 and 3 min following iv metformin. Then, the rats were immediately sacrificed; the liver and kidney were removed and weighed. Concentration of metformin in tissues and plasma were measured. *In vivo* CL_{uptake} was estimated using Eq. (2):

$$CL_{\text{uptake}} = X_{3 \text{ min}} / \text{AUC}_{0-3 \text{ min}} \quad (2)$$

where $X_{3 \text{ min}}$ and $\text{AUC}_{0-3 \text{ min}}$ represent the metformin amount in the tissues at 3 min and AUC up to 3 min following iv metformin, respectively. Effects of Oct2/3 inhibitor corticosterone on *in vivo* uptake of metformin by rat liver were also measured. At 3 min following intraperitoneal dose corticosterone (5 mg/kg) to normal rats, the hepatic uptake of metformin was documented as described above. Dose of corticosterone was cited from previous report³².

2.9. *In vitro* uptake of metformin by primary hepatocytes of rats

In vitro uptake of metformin by primary hepatocytes from experimental rats was documented according to previous report³¹. In brief, the isolated hepatocytes, following 4 h incubation, were incubated in 500 μL of HBSS containing metformin (10, 30 and 100 $\mu\text{mol/L}$, respectively) for 1.5 min referenced as previous report¹⁹ and the uptake reaction was terminated by washing three times with ice-cold HBSS. Intracellular concentrations of metformin were measured by LC-MS/MS method (illustrated in Supporting Information). Effects of Oct1 inhibitor dopamine (20 $\mu\text{mol/L}$) and Oct2/3 inhibitor corticosterone (4 $\mu\text{mol/L}$) on metformin uptake by primary hepatocytes at 100 $\mu\text{mol/L}$ metformin were also measured.

2.10. Cell culture and drug treatment

Caco-2 cells, HK-2 cells and HepG2 cells were seeded in 6-well plates at 1.5×10^5 per well and cultured with high-glucose DMEM medium (for Caco-2 and HepG2) or DMEM/F-12 medium (for HK-2) supplemented with 10% fetal bovine serum in a humidified incubator with 5% CO_2 and 95% O_2 at 37 °C. The mediums were changed every 2 days. When cells reached ~80% confluence, the cells were used for following experiments.

For Caco-2 cells and HK-2 cells, following 48 h incubation with medium containing CDCA (100 $\mu\text{mol/L}$), CA (100 $\mu\text{mol/L}$), DCA (50 $\mu\text{mol/L}$), HDCA (100 $\mu\text{mol/L}$) and GCA (100 $\mu\text{mol/L}$), the cells were collected for measuring expressions of OCT2 protein. The concentrations of bile acids were designed according to previous reports³³. Concentration-dependent effects of CDCA (25, 50 and 100 $\mu\text{mol/L}$), bilirubin (10, 25 and 50 $\mu\text{mol/L}$) and synergistic effect of CDCA (100 $\mu\text{mol/L}$) and bilirubin (50 $\mu\text{mol/L}$) on OCT2 levels were also measured.

For HepG2 cells, the cells were incubated with medium containing different levels of CDCA (25, 50 and 100 $\mu\text{mol/L}$) or bilirubin (1, 10 and 50 $\mu\text{mol/L}$), or CDCA (100 $\mu\text{mol/L}$) plus bilirubin (50 $\mu\text{mol/L}$) for 48 h, the cells were collected for measuring expressions of OCT1 protein. Levels of CDCA and bilirubin were also designed based on pre-experiments. Our pre-experiment showed that expressions of OCT2 protein were not detected in HepG2 cells. Effects of bilirubin and bile acids on expressions of hepatic Oct1 and Oct2 were also investigated in primarily cultured rat hepatocytes. Isolation and culture of primary rat hepatocytes were operated according to previous report³¹ and the cultured cells were treated as described in HepG2 cells.

2.11. Role of FXR activation in CDCA- and bilirubin-regulated expressions of OCT2 in Caco-2 and HK-2 cells

CDCA is considered a natural FXR agonist³⁴. Bilirubin also stimulates FXR³⁵. MCA, an inhibitor of FXR³⁶, was used to

investigate whether CDCA or bilirubin affects the expressions of OCT2 by activating FXR. Caco-2 cells or HK-2 cells were seeded in 6-well plates and exposed to CDCA (100 $\mu\text{mol/L}$), bilirubin (50 $\mu\text{mol/L}$) or another FXR agonist GW4064 (1 $\mu\text{mol/L}$) with or without MCA (100 $\mu\text{mol/L}$) for 48 h.

The role of FXR activation was further confirmed *via* FXR knockdown. Caco-2 cells or HK-2 cells were transfected with FXR siRNA (0.3 nmol/L per well) using lipofectamine® 3000 according to the manufacturer's instructions. The FXR siRNA (Supporting Information Table S3) was designed by GenePharma Technology (Shanghai, China). After 24 h transfection, the cells were incubated in culture medium containing CDCA (100 $\mu\text{mol/L}$), bilirubin (50 $\mu\text{mol/L}$) or GW4064 (1 $\mu\text{mol/L}$) for another 48 h.

2.12. Role of FXR/Fxr activation in CDCA/bilirubin-regulated expressions of OCTs/Octs in HepG2 and primary rat hepatocytes

To investigate roles of FXR activation in regulation of hepatic OCT1/Oct1 and Oct2 protein expressions, HepG2 and primarily cultured rat hepatocytes were treated with CDCA, bilirubin or GW4064 in absence and presence of MCA, respectively. Effects of CDCA, bilirubin or GW4064 on hepatic OCT/Oct protein expressions were further investigated using HepG2 cells transfected using FXR siRNA (0.3 nmol/L per well) and primarily cultured hepatocytes transfected using Fxr siRNA (0.3 nmol/L per well), respectively. The Fxr siRNA was from Thermo Fisher Scientific (Waltham, MA, USA). FXR/Fxr silencing was documented as described above.

2.13. Effects of CDCA treatment on the expressions and function of Octs in intestine, liver and kidney of rats

Rats were treated with CDCA according to previous report³³. Twelve rats were randomly divided into rats treated with CDCA (CDCA) and control (CON) rats. CDCA rats orally received CDCA (180 mg/kg, qd, suspension in 0.5% CMC-Na) for 14 days according to previous report³³. CON rats only received vehicle. The function of intestinal Oct2 in rats was assessed using oral pharmacokinetics of metformin. Protein expressions of intestinal, hepatic and renal Octs in rats as well as levels of CDCA in intestinal contents and plasma of rats were measured at 24 h after the last dose of CDCA.

2.14. Effects of bilirubin treatment on the expressions and function of intestinal, hepatic and renal Octs in rats

Rats were treated with bilirubin according to previous report²³. Twelve rats were randomly divided into rats treated with bilirubin (HB) and control (CON) rats. HB rats received intraperitoneal dose of bilirubin (85.5 $\mu\text{mol/L/kg}$ per day) for 14 days. CON rats only received vehicle. The function of renal Oct2 in rats was assessed using intravenous pharmacokinetics of metformin. Protein expressions of intestinal, hepatic and renal Octs as well as plasma levels of bilirubin in rats were measured at 24 h following the last dose of bilirubin.

2.15. Effect of CDCA treatment and bilirubin treatment on intestinal absorption and urinary excretion of thiamine

Eighteen rats were randomly divided into CON rats, CDCA rats and HB rats. CDCA rats and HB rats received CDCA and bilirubin treatment described above, respectively. On Day 13 of treatment,

6 h urinary samples of each rat were collected and urinary excretions of thiamine were measured. At 24 h after the last dose of CDCA or bilirubin, blood concentration of thiamine and intestinal absorption of thiamine were measured.

2.16. Effects of stigmaterol on the expressions and function of intestinal, hepatic and renal Octs in rats

Stigmaterol, natural antagonist of FXR^{37,38}, was used to further confirm roles of Fxr in expressions of Octs. Twenty four rats were randomly divided into rats treated with control (CON) rats, CDCA rats, stigmaterol (Stig) rats and CDCA plus Stig rats. CDCA rats, Stig rats and CDCA plus Stig rats respectively orally received CDCA (180 mg/kg, qd), Stig (200 mg/kg qd, suspension in 0.5% CMC-Na) and CDCA (180 mg/kg, qd) plus Stig (200 mg/kg qd) for 14 days. CON rats only received vehicle. Stigmaterol dosage was cited from report³⁹. The functions of intestinal and renal Oct2 in rats were assessed using oral and intravenous pharmacokinetics of metformin on Day 13 and Day 14 following dose. Urinary excretion of thiamine, levels of blood thiamine and protein expressions of intestinal, hepatic and renal Octs in rats were measured at 24 h after the last dose.

2.17. Western blot

The protein levels of OCT1/Oct1, OCT2/Oct2, Oct3, Thtr2, Mate1 and FXR/Fxr in rat tissues and targeted cells were measured using Western blot. Samples were obtained by RIPA lysis buffer containing 1 mmol/L phenyl-methyl-sulfonylfluoride. Protein concentrations were determined by a BCA protein assay kit. Equal amounts of proteins were electrophoresed on sodium dodecyl sulfate-polyacrylamide gel (10%) and transferred to nitrocellulose membranes. Protein was blocked in 5% skim milk Tris-buffered saline containing 0.1% Tween 20 (TBST) at room temperature for 1.5 h. The membranes, following washing with TBST, were incubated overnight with corresponding primary antibodies (Supporting Information Table S2) at 4 °C. Following washing with TBST, the membranes were incubated with a horseradish peroxidase-conjugated secondary antibody (Table S2) for 2 h. The protein levels were detected by Tanon high-sig ECL Western blotting substrate (Thermo Fisher Scientific, Waltham, MA, USA) using a gel imaging system (Tanon 5200 Multi Chemiluminescent System, Shanghai, China). All protein levels were normalized to β -actin.

2.18. qRT-PCR analysis

The mRNA levels of Oct1, Oct2, Oct3, Thtr2, Mate1, SHP and FGF19 in tissues or cells were measured using qRT-PCR. Total RNAs were extracted from rat tissues or the indicated using Trizol and used as the template for cDNA synthesis using cDNA Reverse Transcription Kit (ReverTra Ace® qPCR RT Master Mix with gDNA Remover). qRT-PCR was performed on an ABI7500 Fast RT-PCR System (Thermo Fisher, USA) for relative quantification. PCR primer sequences are shown in Supporting Information Table S3. Relative mRNA expressions levels were normalized by β -actin expressions ($2^{-\Delta\Delta Ct}$).

2.19. Immunofluorescence

Paraffin duodenum sections, following deparaffinizing and rehydrating, were incubated in EDTA (0.01 mol/L) antigen

retrieval buffer (pH 8.0) in microwave oven for 15 min. Then the sections were incubated in PBS (pH 7.4) containing 3% hydrogen peroxide at room temperature for 25 min and were blocked in 5% BSA at room temperature for 30 min. Following incubation overnight with rabbit anti-human Oct2 or Oct3 primary antibody (1:75 dilutions) overnight at 4 °C, the sections were incubated with HRP-labeled secondary antibody at room temperature for 50 min and incubated with CY3-TSA fluorescence system kit for another 10 min at room temperature. The sections were heated in a repair box filled with EDTA antigen retrieval buffer (pH 8.0) in microwave oven for 8 min, then turned to low heat for another 7 min to remove the primary and secondary antibodies. Similar processes were operated for the incubation of P-gp primary antibody (1:100 dilution, FITC-TSA labeled fluorescent secondary antibody)/rabbit anti- Na^+/K^+ -ATPase primary antibody (1:100 dilution, CY5 labeled fluorescent secondary antibody) and the secondary antibody. Following washing three times in PBS, the mounting medium containing DAPI was applied; immunofluorescence imaging was performed on the imaging system (Pannoramic).

2.20. PBPK model development

A PBPK model (Supporting Information Fig. S1) characterizing interplays of transporters in intestine, liver and kidney was constructed to describe the pharmacokinetic profiles of metformin in BDL and Sham rats. The essential structure of the model consists of gastrointestinal tract, liver, kidney, portal vein and system compartment. Mass equations are illustrated in Supporting Information materials and methods.

2.21. Statistical analysis

All data are expressed as the mean \pm standard deviation (SD). Phoenix 8.1 (Pharsight, St. Louis, MO, USA) was used for coding and solving of the PBPK model as well as estimating corresponding pharmacokinetic parameters. Statistical analysis among groups was operated using one-way analysis of variance (ANOVA) followed by Sidak's multiple comparisons test. $P < 0.05$ was regarded as statistically significant.

3. Results

3.1. Development of BDL rats

Liver failure rats induced by BDL were confirmed by assessment of physiological and biochemical parameters (Supporting Information Table S4). The results show that BDL significantly increases levels of serum alanine aminotransferase (ALT) and aspartate aminotransferase (AST), accompanied by increases in liver weight. BDL rats exhibit significantly higher plasma levels of both total bile acids and total bilirubin, indicating that the BDL rats may mimic cholestasis in clinical. However, BDL little affected kidney weight, levels of blood urea nitrogen, serum creatinine, 24 h urea protein (Upro/24 h), 24 h urea creatinine and creatinine clearance, inferring that renal function of rats is unaltered. Moreover, BDL rats also show significantly lower levels of blood thiamine ($0.33 \pm 0.03 \mu\text{mol/L}$ in BDL rats *versus* $0.48 \pm 0.03 \mu\text{mol/L}$ in Sham rats, $P < 0.01$), demonstrating thiamine deficiency.

3.2. Pharmacokinetics of metformin in experimental rats after oral or intravenous administration

Plasma concentrations of metformin (Fig. 1A) were determined following oral dose of metformin (40 mg/kg) to experimental rats. Corresponding pharmacokinetic parameters were estimated (Supporting Information Table S5). The results show that peak concentration (C_{\max} , $1.69 \pm 0.04 \mu\text{g/mL}$) and area under curve (AUC, $379.60 \pm 10.06 \mu\text{g min/mL}$) in BDL rats are significantly lower than those (C_{\max} , $4.55 \pm 0.29 \mu\text{g/mL}$ and AUC, $1027 \pm 101.80 \mu\text{g min/mL}$) in Sham rats, but time to peak concentration (T_{\max}) and half-life ($t_{1/2}$) are unaltered. To investigate whether decreases in plasma metformin exposure come from intestinal absorption or renal secretion of metformin, pharmacokinetics of metformin (Fig. 1B and Table S5) was also documented following intravenous dose (10 mg/kg). Significantly decreased plasma metformin exposure is also observed in BDL rats, the estimated AUC ($296.72 \pm 42.12 \mu\text{g min/mL}$) is about 75.4% of Sham rats ($404.5 \pm 19.74 \mu\text{g min/mL}$). The extent of the decreases in AUC of intravenous metformin is less than that of oral metformin, indicating that the decreases in plasma exposure to metformin following oral dose may be due to the integrated effects of the impaired intestinal absorption and the increased renal excretion of metformin. In keeping with the decreases in plasma metformin exposure, treatment with oral metformin no longer shows hypoglycemic effects in BDL rats (Fig. 1C).

3.3. Intestinal absorption of metformin and thiamine as well as expressions of transporters related to intestinal absorption of metformin and thiamine in rats

Absorption of metformin and thiamine in duodenum of rats was documented using *in situ* single-pass perfusion. The results show that BDL remarkably reduces intestinal absorption of metformin in rats (Fig. 1D), whose P_{eff} value is decreased to about 60% of Sham rats. Roles of Oct1, Oct2 and Oct3 in intestinal absorption of metformin were documented using Oct1 inhibitor dopamine, Oct2/3 inhibitor corticosterone and Oct3 inhibitor estradiol, respectively. It is found that corticosterone, but not dopamine nor estradiol, remarkably decreases intestinal absorption of metformin to 60% of control rats (Fig. 1E), indicating that intestinal absorption of metformin is mainly mediated by intestinal Oct2. Intestinal absorption of thiamine in BDL rats was simultaneously measured (Fig. 1F). It is in accordance with the findings in metformin that both BDL and co-administration of corticosterone significantly decrease P_{eff} values of thiamine. mRNA expressions of transporters (Oct1, Oct2, Oct3 and Thtr2) related to intestinal absorption of metformin in duodenum of rats were detected (Fig. 1J). The results showed that BDL significantly downregulates expressions of Oct2 mRNA but not Oct3 nor Thtr2. Expressions of corresponding proteins was also measured (Fig. 1G–I). It is contrast to previous reports^{40,41} that the proteins of Oct1 in the three segments of rat small intestine are not detected. Moreover, expressions of Oct2, Oct3 and Thtr2 protein are regional. Duodenum shows highest expressions of Oct2 and Oct3, followed by jejunum and ileum. Thtr2 protein is only detected in duodenum. Cellular locations of Oct2 and Oct3 protein in duodenum were also identified using immunofluorescence. The results reveal that Oct2 is mainly co-localized with P-gp in the apical membrane (Fig. 1M) although a small amount of Oct2

protein is detected in basolateral membrane of enterocytes. Oct3 protein is mainly located in basolateral membrane (Fig. 1N).

BDL significantly reduces expressions of intestinal Oct2 protein in the three intestinal segments. The expressions of Oct2 protein in duodenum, jejunum and ileum of BDL rats are decreased to 37.4%, 44.0% and 71.8% of Sham rats (Fig. 1G–I), respectively. However, BDL little affected expressions of Oct3 and Thtr2 proteins in intestine of rats. Expressions of Oct2 on duodenum brush-border membrane of rats were also investigated. In line with alterations in expressions of total Oct2 protein, obviously lower expressions of Oct2 protein are detected in intestinal brush-border membrane of BDL rats (Fig. 1K and L).

3.4. Renal excretion of metformin and thiamine as well as expressions of transporters related to renal excretion of metformin in rats

Renal excretions of metformin and thiamine were simultaneously measured to investigate functions of transporters related to renal excretion of metformin. The results show that BDL significantly increases renal secretion of metformin (Fig. 2A) and urinary excretion of thiamine (Fig. 2B). The excretion fraction of metformin and urinary excreted amount of thiamine during 6 h are increased to 125% and 187% of Sham rats, respectively. mRNA and protein expressions of Oct2 and Mate1 in rat kidney were measured (Fig. 2C and D). The results show that BDL significantly upregulates expressions of Oct2 mRNA and protein without affecting expressions of Mate1. The levels of Oct2 protein in kidney of BDL rats is significantly increased to 485% of Sham rats (Fig. 2D), indicating that BDL increases urinary excretion of metformin and thiamine mainly *via* increasing expressions of renal Oct2 protein. It was in line with the deduction that BDL also significantly increases uptake of metformin in renal slice (Fig. 2E). The *in vivo* renal uptake clearance of metformin in BDL rats is also significantly increased to 2-fold of Sham rats (Fig. 2F).

3.5. Expressions and function of Octs in rat liver

mRNA and protein expressions of Octs in rat liver were measured (Fig. 2G and H). The results show that BDL significantly downregulates mRNA expressions of Oct1 and upregulates mRNA expressions of Oct2 without affecting mRNA expressions of Oct3. Proteins Oct1 and Oct2 but not Oct3 are detected in rat liver, although levels of Oct2 protein are less than Oct1 (Fig. 2H). It is in line with alterations in mRNA expressions of Octs that BDL downregulates expressions of Oct1 (Fig. 2H) but upregulates expressions of Oct2 protein, which are altered to be 0.5- and 3.9-fold of Sham rats, respectively. Functions of Octs were documented using both *in vivo* and *in vitro* uptake of metformin. The results show that BDL significantly downregulates expressions of hepatic Oct1, but little affects *in vivo* uptake of metformin (Fig. 2I), which may be partly attributed to induction of hepatic Oct2. *In vitro* data also demonstrate that uptake of metformin by primarily cultured hepatocytes from BDL rats is similar to that by Sham rats (Fig. 2J). Roles of hepatic Oct1 and Oct2 *in vitro* uptake of metformin by hepatocytes were also investigated in presence of Oct1 inhibitor dopamine and Oct2/3 inhibitor corticosterone (Fig. 2K). In Sham rats, dopamine and corticosterone show similar inhibition on hepatic uptake of metformin (58.7% for dopamine and 50.5% for corticosterone). However, in BDL rats, inhibition of dopamine on hepatic uptake of metformin is obviously weakened

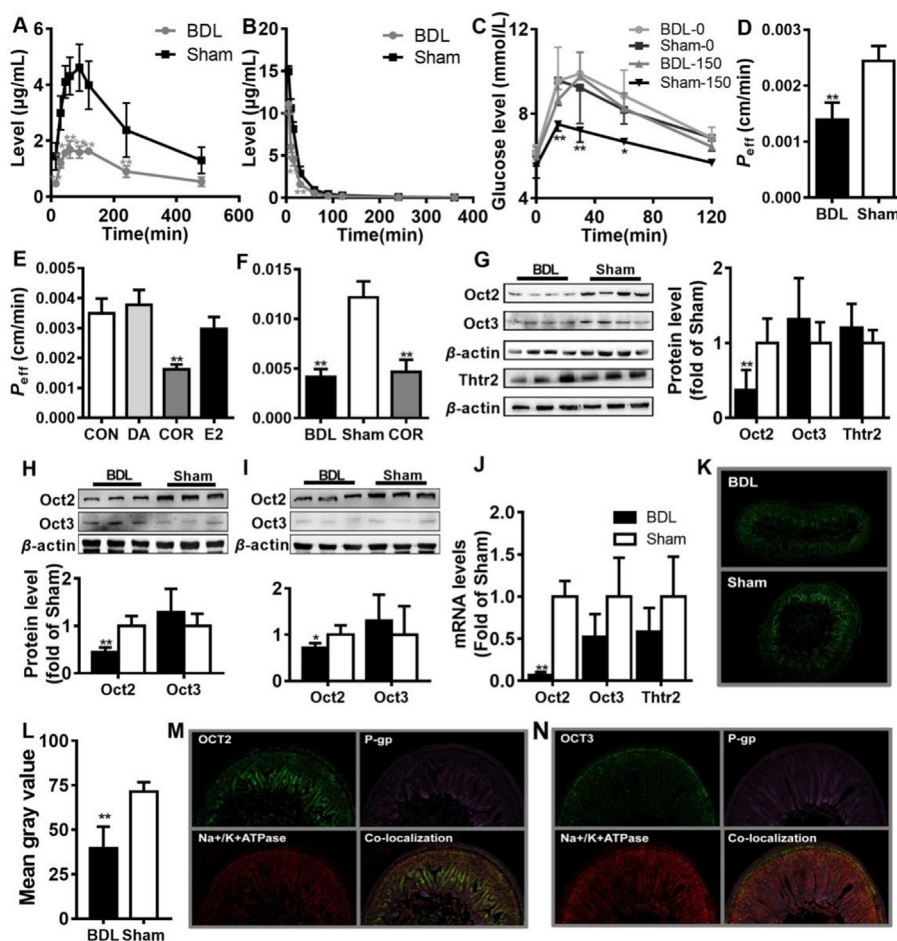


Figure 1 Effects of BDL on function of Octs in intestine of rats. (A–B) Plasma concentrations of metformin following oral administration of metformin (40 mg/kg) (A) ($n = 6$) and following intravenous administration of metformin (10 mg/kg) (B) ($n = 5$) to BDL and Sham rats. (C) Blood glucose levels following oral 2 g/kg glucose to BDL rats and Sham rats treated with or without 150 mg/kg metformin ($n = 5$). (D) P_{eff} values of metformin in duodenum of BDL and Sham rats ($n = 6$). (E) P_{eff} values of metformin in intestine of Sham rats co-administrated with dopamine (DA), corticosterone (COR) and estradiol (E2) ($n = 5$). (F) P_{eff} values of thiamine in intestine of BDL and Sham rats as well as Sham rats co-administrated with corticosterone ($n = 6$). (G–I) Protein levels of Oct2, Oct3 and Thtr2 in the duodenum (G, $n = 8$), jejunum (H, $n = 6$) and ileum (I, $n = 6$) of BDL and Sham rats. (J) mRNA levels of Oct2, Oct3 and Thtr2 in the duodenum of BDL and Sham rats ($n = 6$). (K–L) Expressions of Oct2 protein on duodenum brush-border membrane of BDL and Sham rats. (M–N) Oct2 (M) and Oct3 (N) co-localization with P-gp or Na⁺/K⁺ ATPase in duodenum of BDL and Sham rats. Data are expressed as mean \pm SD. * $P < 0.05$, ** $P < 0.01$ vs Sham rats.

from 58.7% in Sham rats to 25.2% in BDL rats. On the contrast, inhibition of corticosterone on metformin uptake is remarkably enhanced from 50.5% in Sham rats to 80.6% in BDL rats. The results indicate that contribution of hepatic Oct1 to hepatic uptake metformin in BDL rats is decreased while contribution of Oct2 is enhanced, which are in line with the decreased Oct1 expressions and the increased Oct2 expressions. Roles of Oct2 protein in hepatic disposition of metformin were further documented in normal rats treated with corticosterone. The results show that it is consistent with *in vitro* data that co-administration of corticosterone significantly decrease *in vivo* hepatic uptake clearance of metformin, which was decreased to 50% of CON rats (Fig. 2L).

3.6. Both bile salts and bilirubin induce expressions of OCT2 protein in Caco-2 cells and HK-2 cells

In vivo data show that levels of bile salts in intestinal contents of BDL rats are significantly lower than those of Sham rats (Fig. 3A).

Significantly increases in levels of DCA and HDCA are also observed in plasma of BDL rats (Fig. 3B). Levels of bile salts in liver and kidney of rats were also measured. Obviously increased DCA levels (Fig. 3C) and GCA levels (Fig. 3D) are detected in liver and kidney of BDL rats, respectively. Bilirubin level in intestinal contents of BDL rats shows a mild decrease trend, but no significance is obtained (Fig. 3E). Significantly increased plasma levels of bilirubin are found in liver, kidney and plasma of BDL rats (Fig. 3E). The results indicate that the decreased levels of bile salts in intestine and the increased plasma levels of bilirubin may become factors that BDL differently regulates the protein expressions of Octs in intestine and kidney of rats. To confirm the above deduction, effects of bile salts and bilirubin on expressions of OCT2 protein in Caco-2 cells and HK-2 cells were investigated. The results show that among tested 5 bile salts (DCA, CDCA, HDCA, CA and GCA), only CDCA remarkably induces expressions of OCT2 in Caco-2 cells (Fig. 3F). Further investigation shows that both CDCA (Fig. 3G) and bilirubin (Fig. 3H)

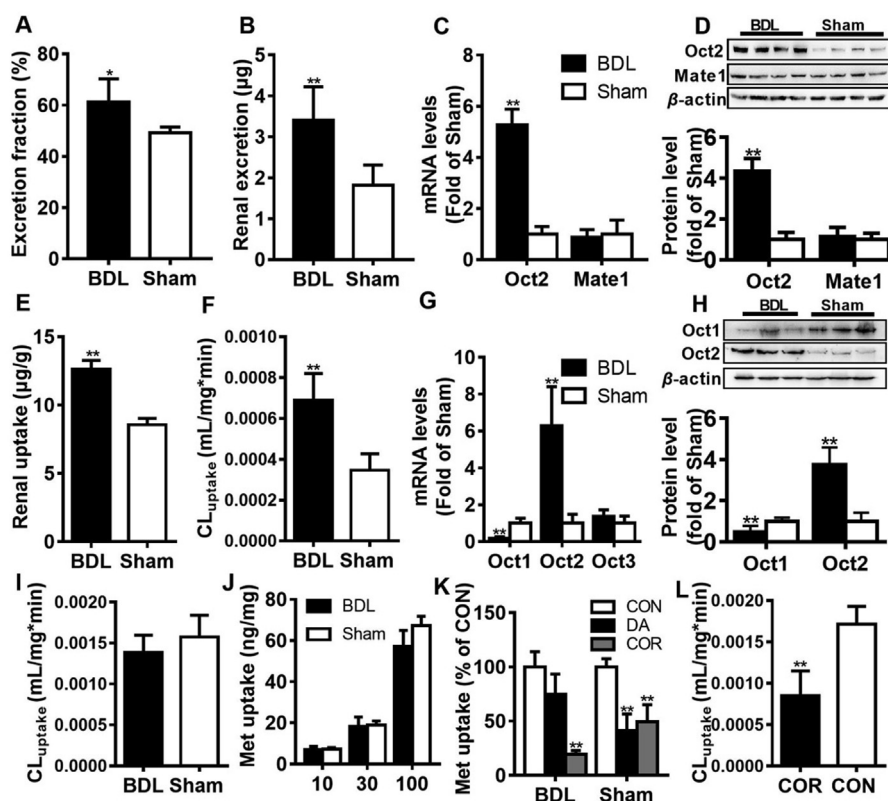


Figure 2 Effects of BDL on function of Octs in liver and kidney of rats. (A) Excretion fraction of metformin during 6 h in BDL and Sham rats ($n = 5$). (B) Renal excretion of thiamine during 6 h in BDL and Sham rats ($n = 6$). (C) mRNA levels of Oct2 and Mate1 in the kidney ($n = 6$) of BDL and Sham rats. (D) Protein expressions of Oct2 and Mate1 in kidney of BDL and Sham rats ($n = 8$). (E) Uptake of metformin in renal slice of BDL and Sham rats ($n = 6$). (F) The *in vivo* uptake clearance (CL_{uptake}) by rat kidney ($n = 6$). (G) mRNA levels of Oct1, Oct2 and Oct3 in liver of BDL and Sham rats ($n = 6$). (H) Protein expressions of Oct1 and Oct2 in liver of BDL and Sham rats ($n = 6$). (I) The *in vitro* CL_{uptake} by liver of BDL and Sham rats ($n = 6$). (J) The *in vitro* uptake of metformin by the primary hepatocytes from BDL and Sham rats ($n = 6$). (K) Effects of dopamine (DA) and corticosterone (COR) on uptake of metformin by the primary hepatocytes from BDL and Sham rats (% of control cells, $n = 6$). (L) Effects of corticosterone on CL_{uptake} of metformin in liver of normal rats ($n = 6$). Data are expressed as mean \pm SD. * $P < 0.05$, ** $P < 0.01$ vs Sham rats or control (CON) cells or rats.

concentration-dependently increase expressions of OCT2 in Caco-2 cells. Interestingly, although both CDCA and bilirubin upregulate expressions of OCT2 in Caco-2 cells (Fig. 3I), neither cooperative effect nor additive effect is observed. The findings in Caco-2 cells are completely repeated in HK-2 cells (Fig. 3J–M). These results indicate that downregulation of intestinal OCT2 protein by BDL is mainly attributed to decreases in levels of intestinal bile salts and that upregulation of renal OCT2 protein by BDL is possibly owed to the increased plasma levels of bilirubin in plasma and kidney.

3.7. Involvement of FXR activation in induction of OCT2 protein in Caco-2 and HK-2 cells by CDCA and bilirubin

Bile salts and bilirubin, the natural ligands of FXR, show their biological effects *via* activating FXR^{42,43}. CDCA was also reported to suppress hepatic OCT1 *via* FXR activation⁴². To investigate whether induction of OCT2 expressions in Caco-2 and HK-2 cells are involved in FXR activation, effects of bilirubin and CDCA on expressions of OCT2 protein in the indicated cells were documented using both the FXR inhibitor MCA and FXR siRNA. Another FXR agonist GW4064 served as positive control. The results show that bilirubin, CDCA and GW4064 all induce

expressions of OCT2 protein in Caco-2 cells (Fig. 4A–C), which are remarkably attenuated by MCA. To confirm the roles of FXR activation in CDCA- and bilirubin-mediated upregulation of OCT2 expressions, FXR in Caco-2 cells was silenced using FXR siRNA. Western blotting shows that expressions of FXR protein in Caco-2 transfected with FXR siRNA is decreased to 33% of control cells (Fig. 4D), demonstrating successful silencing of FXR. FXR siRNA itself suppresses the expressions of OCT2 protein in Caco-2 (Fig. 4E) cells. Furthermore, FXR siRNA remarkably attenuates the induction of OCT2 protein expressions by CDCA and bilirubin (Fig. 4F). GW4064 no longer upregulates the expressions of OCT2 protein in Caco-2 transfected with FXR siRNA (Fig. 4G). The results in Caco-2 cells are almost repeated in HK-2 cells (Fig. 4H–N). Short heterodimer partner (SHP) and fibroblast growth factor 19 (FGF19) are considered to be targeted genes of FXR³³, expressions of the two genes were measured in HK-2 cells to investigate whether FXR is activated or inhibited (Fig. 4O). It is consistent with our expectation that CDCA, GW4064 and bilirubin significantly upregulate expressions of SHP and FGF19 mRNA. MCA significantly downregulates expressions of SHP mRNA and slight inhibits expressions of FGF19 mRNA. All these results demonstrate that FXR is activated by CDCA, GW4064 and bilirubin, while FXR is inhibited by MCA.

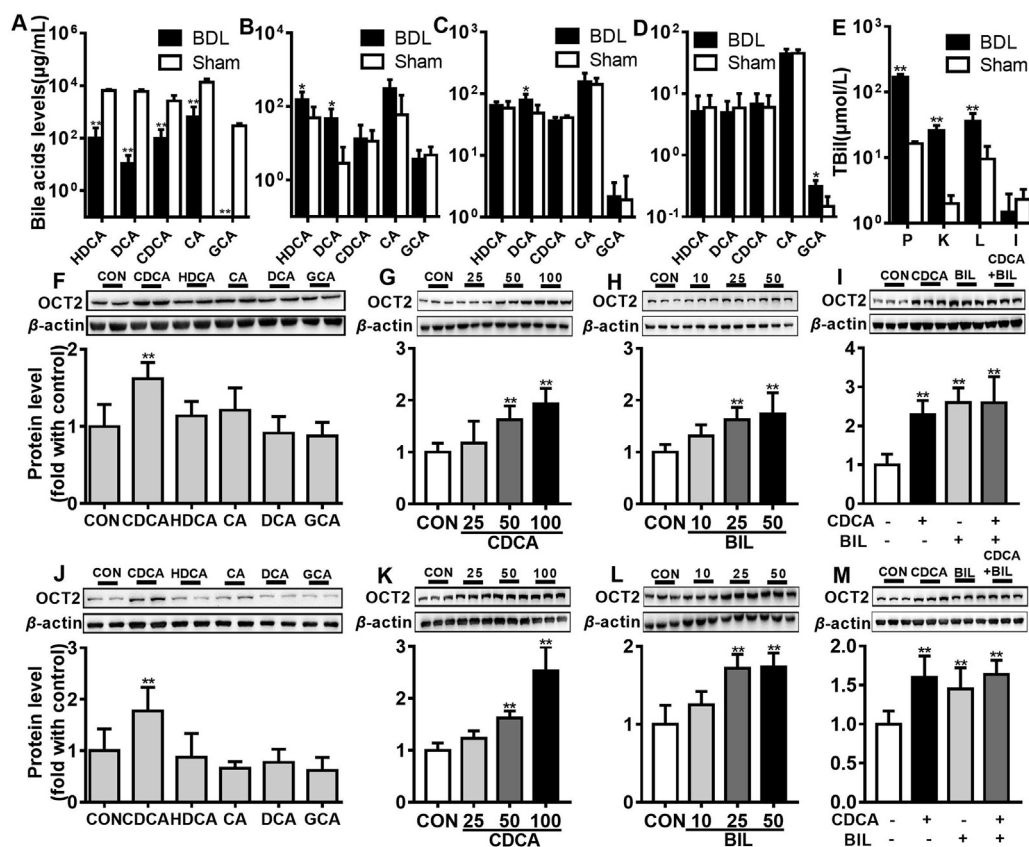


Figure 3 Effects of bile salts and bilirubin on expressions of OCTs protein in Caco-2 and HK-2. (A–D) Levels of CDCA, HDCA, CA, DCA and GCA in intestinal contents (A), plasma (B), liver (C) and kidney (D) of BDL and Sham rats. (E) Levels of total bilirubin (TBil) in intestinal contents (I), liver (L), kidney (K) and plasma (P) of BDL rats and Sham rats. (F) Effects of CDCA, HDCA, CA, DCA and GCA on expressions of OCT2 protein in Caco-2 cells; (G–I) Concentration-dependent effects of CDCA (G) and bilirubin (BIL, H) on expressions of OCT2 protein as well as their combined effects (I). (J) Effects of CDCA, HDCA, CA, DCA and GCA on expressions of OCT2 protein in HK-2; (J–M) Concentration-dependent effects of CDCA (J) and BIL (L) on expressions of OCT2 protein as well as their combined effects (M) in HK-2 cells. Data are expressed as mean \pm SD ($n = 6$). * $P < 0.05$, ** $P < 0.01$ vs Sham rats or control (CON) cells.

These results indicate that CDCA and bilirubin induce expressions of OCT2 protein in Caco-2 cells and HK-2 cells *via* activating FXR. Effects of CDCA, GW4064 and bilirubin on expressions of FXR protein in HK-2 cells were also investigated. It is observed that CDCA, and bilirubin but not GW4064 can induce expressions of FXR protein (Fig. 4P). In line with this issue, significantly lower expressions of intestinal Fxr protein (Fig. 4Q) and higher expressions of renal Fxr protein (Fig. 4R) are observed in BDL rats.

3.8. Both CDCA and bilirubin downregulate expressions of OCT1 protein in HepG2 and oppositely regulate expressions of Oct2 and Oct1 protein in primary rat hepatocytes *via* FXR activation

In vivo data show that BDL downregulates expressions of hepatic Oct1 protein but upregulates expressions of hepatic Oct2 protein. In line with *in vivo* finding, both CDCA (Fig. 5A) and bilirubin (Fig. 5B) concentration-dependently downregulate expressions of OCT1 protein in HepG2 cells, but CDCA and bilirubin do not show cooperative effect or additive effect (Fig. 5C). Similarly, GW4064 also downregulates the expressions of OCT1 protein (Fig. 5F). Decreases in expressions of OCT1 by CDCA (Fig. 5D),

bilirubin (Fig. 5E) and GW4064 (Fig. 5F) are remarkably reversed by MCA. Roles of FXR in expressions of OCT1 were further investigated using silencing FXR HepG2 cells. Expressions of FXR protein in silencing FXR HepG2 cells are significantly downregulated, demonstrating successful silencing of FXR (Fig. 5G). Silencing FXR itself upregulates expressions of OCT1 protein in HepG2 cells (Fig. 5H–J) and almost abolishes downregulation of OCT1 protein by CDCA (Fig. 5H), bilirubin (Fig. 5I) and GW4064 (Fig. 5J). OCT2 protein is not detected in HepG2 cells. Thus, effects of CDCA and bilirubin on expressions of Oct1 and Oct2 protein were measured using primarily cultured rat hepatocytes. The results show that CDCA (Fig. 5K), bilirubin (Fig. 5L) and GW4064 (Fig. 5M) downregulate expressions of Oct1 protein but upregulate expressions of Oct2 protein in primarily cultured rat hepatocytes, which is remarkably attenuated by MCA. To further confirm roles of Fxr in expressions of hepatic Oct1 and Oct2 protein, expressions of Fxr in primarily cultured rat hepatocytes are successfully silenced (Fig. 5G). As expectation, silencing Fxr itself increases expressions of Oct1 protein and downregulates expressions of Oct2 protein in primarily cultured rat hepatocytes. CDCA (Fig. 5Q), bilirubin (Fig. 5R) and GW4064 (Fig. 5S) no longer alter expressions of Oct2 and Oct1 protein in primarily cultured rat hepatocytes transfected siRNA Fxr. High

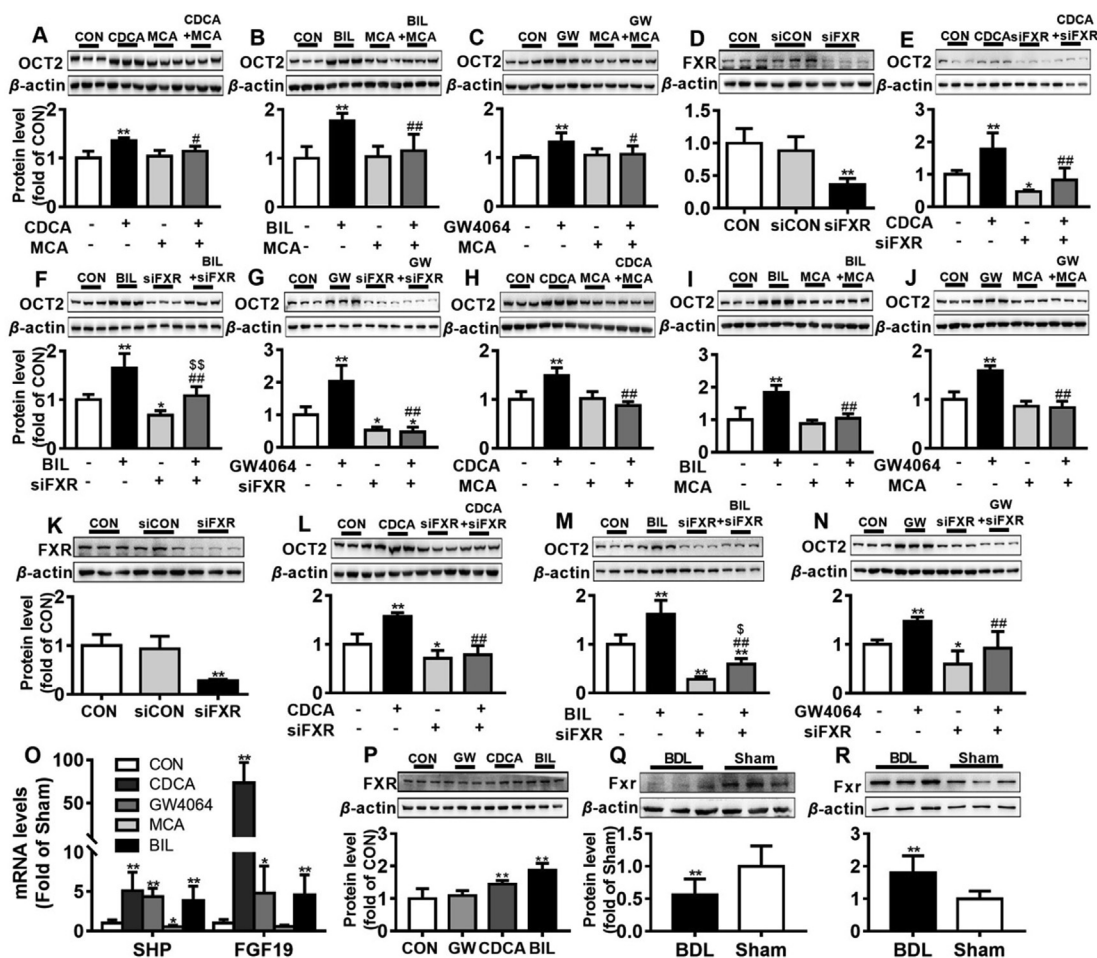


Figure 4 Effects of glycine- β -muricholic acid (MCA) and FXR knockdown on expressions of OCT2 protein mediated by CDCA or bilirubin (BIL) in Caco-2 and HK-2 cells. (A–C) Effects of MCA on expressions of OCT2 protein by CDCA (A), BIL (B) and GW4064 (C) in Caco-2 cells; (D) Effect of FXR knockdown on FXR expressions in Caco-2; (E–G) Effect of FXR knockdown on expressions of OCT2 protein mediated by CDCA (E), bilirubin (F) and GW4064 (G) in Caco-2 cells. (H–J) Effects of MCA on expressions of OCT2 protein by CDCA (H), bilirubin (I) and GW4064 (J) in HK-2 cells; (K) Effect of FXR knockdown on FXR expressions in HK-2 cells; (L–N) Effect of FXR knockdown on expressions of OCT2 protein mediated by CDCA (L), BIL (M) and GW4064 (N) in HK-2 cells. (O) Effects of CDCA, BIL and GW4064 on mRNA levels of SHP and FGF19 in HK-2 cells. (P) Effects of CDCA, BIL and GW4064 on levels of FXR in HK-2 cells; (Q–R) Expressions of Fxr protein in duodenum (Q) and kidney (R) of BDL and Sham rats. Data are presented as the mean \pm SD ($n = 6$). * $P < 0.05$ and ** $P < 0.01$ vs control (CON) cells or Sham rats. # $P < 0.05$ and ## $P < 0.01$ vs CDCA, BIL or GW4064, $^{\$}P < 0.05$ vs siFXR.

levels of bilirubin are observed in liver of BDL rats, indicating that opposite regulations of hepatic Oct1 and Oct2 by BDL are attributed to the increased levels of bilirubin and that bilirubin oppositely regulates expressions of Oct1 and Oct2 protein *via* Fxr activation. Significantly higher expressions of Fxr protein are also observed in liver of BDL rats (Fig. 5T).

3.9. Effects of CDCA treatment and bilirubin treatment on pharmacokinetics of metformin and expressions of drug transporters related to metformin in intestine, kidney and liver rats

To further investigate roles of intestinal CDCA in expressions of intestinal Oct2 protein, rats were treated with oral dose of CDCA for 14 days. Significantly increases levels of CDCA are detected in intestinal contents and plasma of rats (Fig. 6A). Pharmacokinetics of oral metformin and expressions of Oct protein in intestine, liver and kidney of rats were also measured. The results show that

CDCA treatment significantly increases plasma metformin exposure (Fig. 6B and Table S5), the estimated C_{max} and AUC values are $4.36 \pm 0.38 \mu\text{g/mL}$ and $906.85 \pm 52.16 \mu\text{g min/mL}$ respectively, significantly higher than those (C_{max} , $3.19 \pm 0.12 \mu\text{g/mL}$ and AUC, $707.20 \pm 30.01 \mu\text{g min/mL}$) in control rats. Significantly upregulated expressions of intestinal Oct2 (Fig. 6C) are observed in intestine of rats treated with CDCA. However, expressions of intestinal Oct3 (Fig. 6C), intestinal Thtr2, hepatic Oct1, hepatic Oct2 (Fig. 6D), renal Oct2 and renal Mate1 (Fig. 6E) are unaltered.

Roles of bilirubin in expressions of renal Oct2 and hepatic Oct1/Oct2 were also documented using rats treated with intraperitoneal bilirubin for 14 days. The rats treated with bilirubin show remarkably higher levels of serum bilirubin (Fig. 6F), demonstrating successful development of hyperbilirubinemia rats. Pharmacokinetic analysis shows that treatment with bilirubin significantly decreases plasma metformin exposure following

intravenous administration (Fig. 6G and Table S5), the estimated AUC significantly is $220.07 \pm 16.31 \mu\text{g min/mL}$, which is significantly lower than that ($410.12 \pm 57.74 \mu\text{g min/mL}$) in control rats. Further study shows that although treatment with bilirubin does not alter expressions of intestinal Oct2, Oct3 and Thtr2 protein (Fig. 6H), treatment with bilirubin significantly induces expressions of hepatic Oct2 (Fig. 6I) and renal Oct2 (Fig. 6J) but lowers expressions of hepatic Oct1 protein (Fig. 6J).

3.10. Effects of CDCA treatment or bilirubin treatment on intestinal absorption of thiamine and renal excretion

Disposition of thiamine in CDCA-treated and bilirubin-treated rats is measured. It is in line with alterations in expressions of intestinal and renal Oct2 protein that CDCA but not bilirubin treatment significantly increases intestinal absorption (Fig. 6K). On the contrast, bilirubin but not CDCA increases 6h renal excretions of thiamine (Fig. 6L). Fasting blood levels of thiamine were also measured (Fig. 6M). It is in line with alterations in intestinal absorption and renal excretion of thiamine that CDCA-treated rats show higher blood levels of thiamine and that obviously lower blood levels of thiamine are observed in bilirubin-treated rats.

3.11. Effects of stigmasterol on the expressions and function of intestinal, hepatic and renal Oct2 in rats

Whether stigmasterol antagonizes CDCA-activated FXR was also documented using HepG2 cell. The results show that stigmasterol ($100 \mu\text{mol/L}$) little affects mRNA expressions of SHP and FGF19, targeted genes of FXR, but co-administration of stigmasterol significantly reversed the upregulation mRNA expressions of SHP and FGF19 by CDCA, confirming that stigmasterol antagonizes CDCA-activated FXR (Fig. 6N). *In vivo* study shows that oral administration of stigmasterol itself decreases expressions of intestinal Oct2 protein (Fig. 6Q), leading to significant decrease in plasma exposure of metformin (Fig. 6O and Supporting Information Table S6) following oral dose. Oral administration of stigmasterol also attenuates the increased expressions of intestinal Oct2 protein (Fig. 6Q) and plasma exposure of metformin following oral dose by CDCA administration (Fig. 6O). The CDCA-induced increase in levels of blood thiamine is also attenuated by stigmasterol (Fig. 6T). Oral administration of stigmasterol little affects expressions of renal and hepatic Oct proteins (Fig. 6R and S) as well as pharmacokinetics of metformin following intravenous dose (Fig. 6P and Table S6).

3.12. Prediction of metformin pharmacokinetics following oral or intravenous administration of metformin in BDL and sham rats using the Semi-PBPK model

The semi-PBPK model was developed to predict pharmacokinetic profiles after intravenous dose (10 mg/kg) (Fig. 7A) and oral dose (40 mg/kg) (Fig. 7B) of metformin to BDL and Sham rats based on parameters listed in Table 1. In addition to alterations in expressions of Oct protein, liver failure also alters some physiological parameters such as liver volume, hepatic blood flow, and renal blood flow, gastrointestinal transit time, which may affect pharmacokinetic behaviors of metformin and are also introduced into the PBPK stimulation (Table 1). It is assumed that alterations in functions of intestinal Oct2, renal Oct2 and hepatic Oct1/Oct2 by BDL are related to alterations in their protein expressions, thus, the transporter-mediated parameters ($P_{\text{eff, Oct2}}$ or $CL_{\text{int, Oct1}}$) under

BDL status were corrected by the alterations in protein expressions of Oct2. Plasma concentration profiles of metformin following oral or intravenous dose to BDL and Sham rats are predicted (Fig. 7A and B) and corresponding pharmacokinetic parameters are estimated (Supporting Information Table S7). The developed semi-PBPK model was also used to predict pharmacokinetic profiles of metformin in bilirubin-treated rats (Fig. 7C) and CDCA-treated rats (Fig. 7D). It is generally accepted that the predictions are considered successful if the ratio of prediction to observation falls between 0.5 and 2.0⁵⁷. The results show that both most (63/65) of the predicted concentrations of metformin (Fig. 7E) and all of the predicted pharmacokinetic parameters (Table S7) are within 0.5–2.0-fold of observations, demonstrating that pharmacokinetics of metformin in the experimental rats are successfully predicted.

Sensitivity analysis is documented to investigate individual contributions of alterations in gastric emptying rate (Fig. 7F), intestinal transit rate (Fig. 7G), intestinal Oct2 (Fig. 7H), renal Oct2 (Fig. 7I), renal blood flow (Fig. 7J), hepatic Oct1 (Fig. 7K) and hepatic blood (Fig. 7L) to plasma metformin exposure following oral dose. Alterations in gastric emptying rate, intestinal transit rate, renal blood flow and hepatic blood were set to be 0.5-, 1.0- and 2.0-fold, but alterations for Oct2 and Oct1 were set to be 0.1-, 1.0- and 10.0-fold. The results show that individual contributions (AUC) of alterations are intestinal Oct2 > renal Oct2 > intestinal transit rate > gastric emptying rate > renal blood flow. Contributions of both hepatic Oct1 and hepatic blood flow are minor. Mimicked analysis also demonstrates that altered pharmacokinetic behavior of metformin by BDL is attributed to integrated effects of decreased intestinal Oct2, increased renal Oct2, decreased gastric emptying rate, decreased intestinal transport rate and decreased renal blood flow in BDL rats (Fig. 7M). More importantly, decreases in gastric emptying rate and decreases in intestinal transit rate show opposite effects on oral plasma metformin exposure. The predicted levels of metformin following oral dose in liver of BDL rats are obviously lower than that in Sham rats (Fig. 7N), which may partly explain disappearance of metformin hypoglycemic effects. Lower levels of hepatic Oct1 protein and increased hepatic Oct2 protein expressions are observed in the liver of BDL rats. Simulation analysis shows that contributions of the decreased hepatic Oct1 protein to hepatic levels of metformin are partly abolished by the increased hepatic Oct2 protein (Fig. 7N); their net effects are to increase levels of hepatic metformin, indicating that the low levels of metformin in liver of BDL rats mainly come from the decreased plasma levels of metformin.

The developed Semi-PBPK model is also successfully used to predict plasma concentrations of metformin in ethynylestradiol-induced cholestasis rats (Fig. S2A). The predicted metformin in liver of the cholestasis rats was obviously lower than those in control rats (Fig. S2B), which may partly explain that antidiabetic effect of metformin, is impaired in ethynylestradiol-induced cholestasis rats¹⁹. The developed Semi-PBPK model is tried to predict pharmacokinetics of metformin in healthy subjects and patients (Fig. S3). The predicted plasma concentrations of metformin following oral dose (250 or 850 mg) of metformin are within 0.5–2.0-fold of clinic observations, inferring that developed Semi-PBPK mode in rats is also suitable for human. Simulations shows that plasma and hepatic concentrations of metformin in patients with liver failure are remarkably lower than those in healthy subjects, indicating that liver failure may impair hypoglycemic effect of metformin, which needs further clinical investigation.

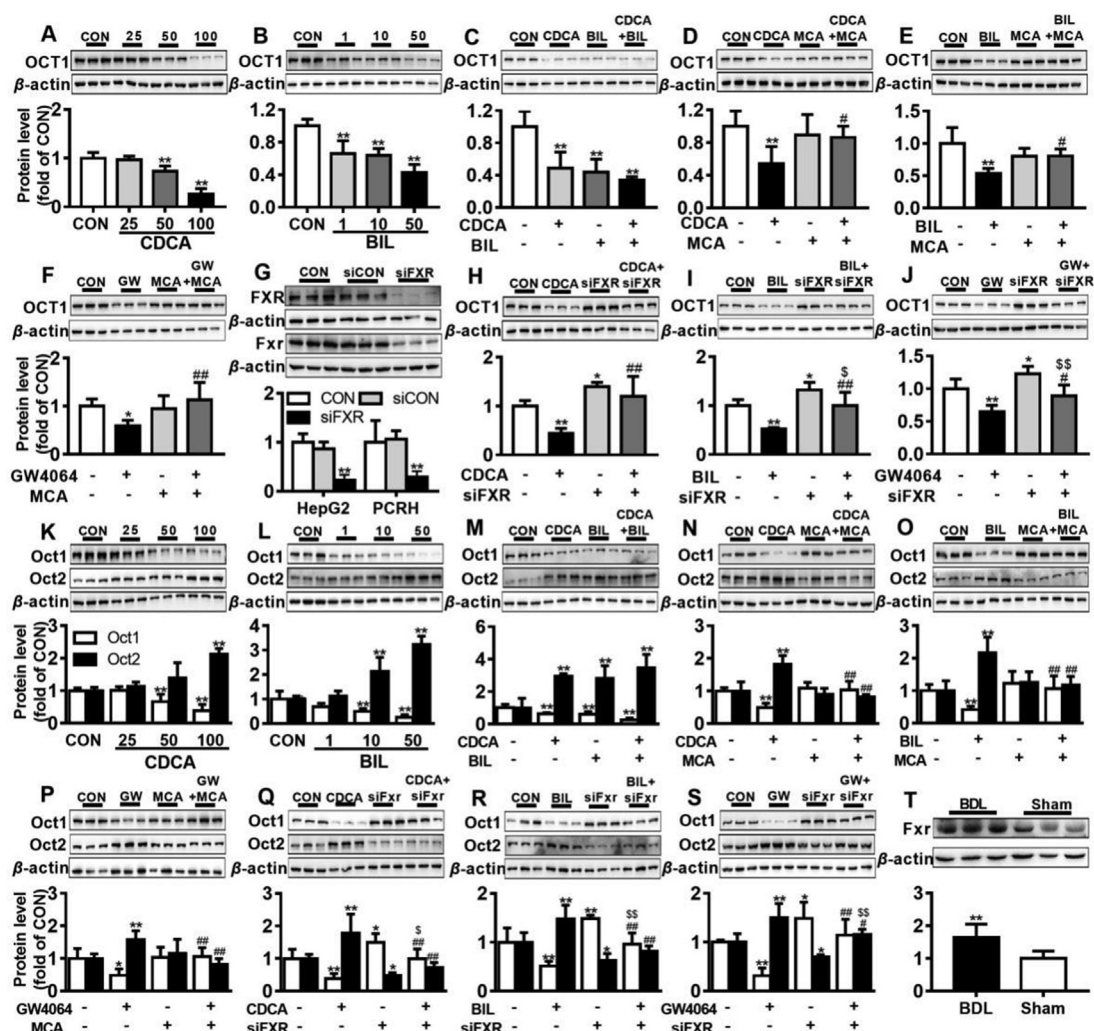


Figure 5 Effects of CDCA and bilirubin (BIL) on expressions of OCT1 protein in HepG2 cells as well as Oct1 and Oct2 in primarily cultured rat hepatocytes. (A–C) Effects of CDCA (A), bilirubin (B) and CDCA + BIL (C) on expressions of OCT1 protein in HepG2 cells. (D–F) Effects of MCA on downregulation of OCT1 protein by CDCA (D), BIL (E) and GW4064 (F) in HepG2 cells. (G) Effect of FXR/Fxr knockdown on FXR/Fxr expressions in HepG2 cells and primarily cultured rat hepatocytes (PCRH). (H–J) Effect of FXR knockdown on down regulation of OCT1 protein by CDCA (H), BIL (I) and GW4064 (J). (K–M) Effects of CDCA (K) and BIL (L) and CDCA + BIL (M) on expressions of Oct1 and Oct2 protein in primarily cultured rat hepatocytes. (N–P) Effects of MCA on the altered expressions of Oct1 and Oct2 protein by CDCA (N), BIL (O) and GW4064 (P) in primarily cultured rat hepatocytes. (Q–S) Effect of Fxr knockdown on alterations in expressions of Oct1 and Oct2 protein by CDCA (Q), BIL (R) and GW4064 (S) in primarily cultured rat hepatocytes. (T) Expressions of Oct1 and Oct2 protein in liver of BDL and Sham rats. Data are presented as the mean \pm SD ($n = 6$). * $P < 0.05$ and ** $P < 0.01$ vs control (CON) cells or Sham rats. # $P < 0.05$ and ## $P < 0.01$ vs CDCA, BIL or GW4064, $^{\$}P < 0.05$ and $^{\$\$}P < 0.01$ vs siFxr.

4. Discussion

Several studies have demonstrated that liver injury alters expressions of OCTs in liver and kidney, which are dependent on type of liver failure and OCT species. For example, liver injury induced by ischemia–reperfusion downregulates expressions of renal Oct2 and Mate1, leading to decreases in systemic and tubular secretory clearance of cimetidine²⁰. Significant downregulation of hepatic Oct1 and renal Oct2 are also observed in ethynylestradiol-induced cholestasis rats¹⁹. It is consistent with our study that BDL downregulates hepatic Oct1 expressions⁵⁸ but upregulates expressions of renal Oct2 without affecting expressions of renal Mate1²⁰. Significant decrease in OCT1 is detected in liver donors diagnosed as cholestatic⁵⁹. To our knowledge, this is the first

systematic report that BDL downregulates expressions of intestinal Oct2 and hepatic Oct1 protein but upregulates expressions of renal Oct2 and hepatic Oct2 protein, leading to significant decreases in plasma metformin exposure to following oral and intravenous dose, diminishing antidiabetic effect of metformin. Real mechanisms that BDL differently regulates protein expressions of OCTs in intestine, liver and kidney were further investigated using Caco-2, HepG2 and HK-2 cells.

Metformin, almost not metabolized by the liver or excreted by bile, eliminates mainly *via* urine, whose renal clearance is 4 times larger than glomerular filtration rate²⁶, indicating existence of renal secretion. Metformin transport is mainly mediated by OCTs, MATEs¹ and THTRs¹³. Here, metformin serves as a model drug to assess functions of these transporters. Pharmacokinetic analysis

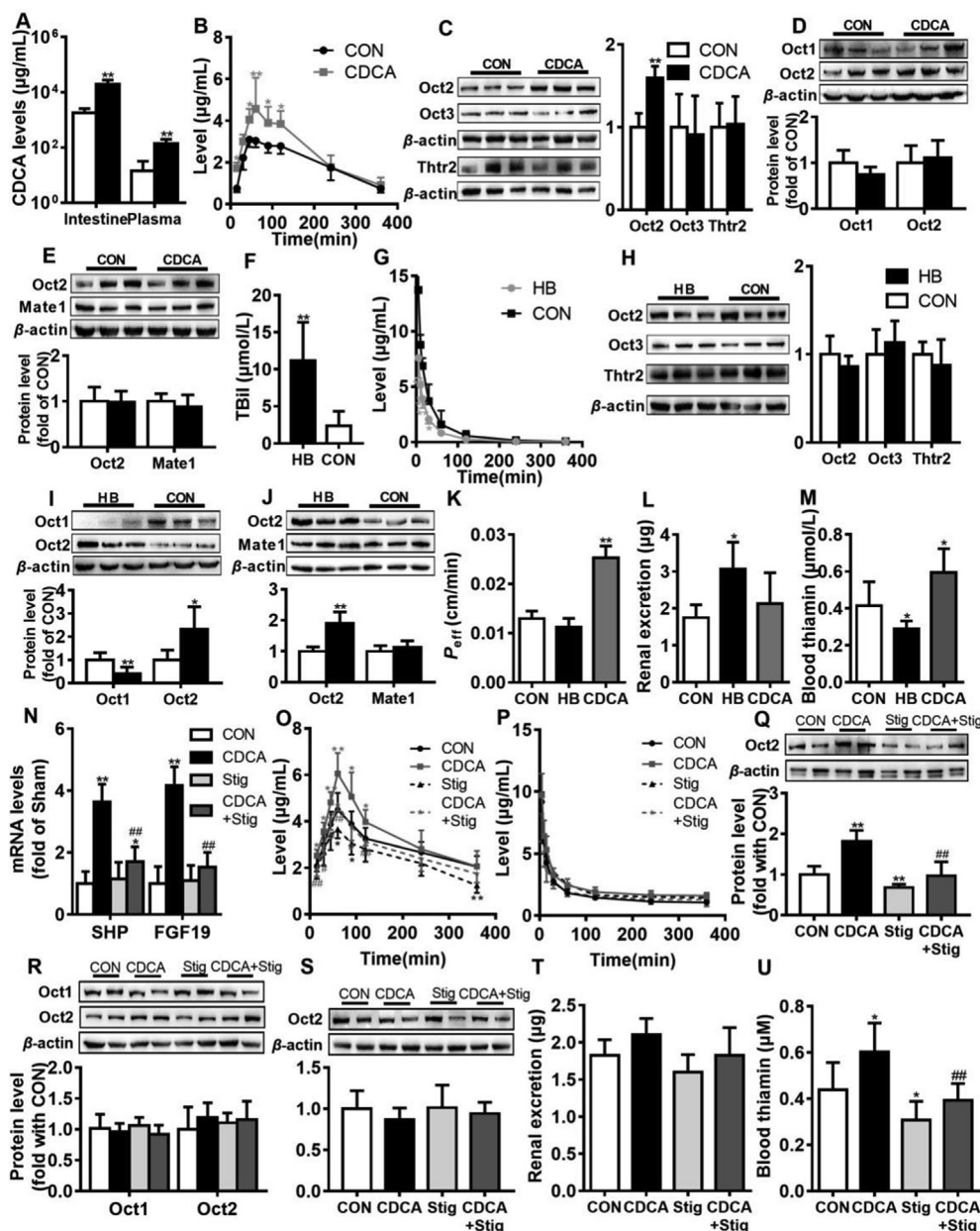


Figure 6 Effects of CDCA, bilirubin and stigmaterol (Stig) on expressions and function of Oct2 in intestine and kidney of rats. (A) Levels of CDCA in intestinal contents and plasma of control (CON) and CDCA-treated (CDCA) rats. (B) Plasma concentrations of metformin following oral administration of metformin (40 mg/kg) to CON and CDCA rats. (C) Protein expressions of intestinal Oct2, Oct3 and Thtr2, (D) protein expressions of hepatic Oct1 and Oct2, (E) protein expressions of renal Oct2 and Mate1 in CON and CDCA rats. (F) Levels of bilirubin in serum of CON and bilirubin-treated (HB) rats. (G) Plasma concentrations of metformin following intravenous administration (10 mg/kg) to CON and HB rats. (H) Protein expressions of intestinal Oct2, Oct3 and Thtr2, (I) protein expressions of hepatic Oct1 and Oct2, (J) protein expressions of renal Oct2 and Mate1 in CON and HB rats. (K) P_{eff} values of thiamine in intestine of CON, CDCA and HB rats. (L) Renal excretion of thiamine during 6 h in CON, CDCA and HB rats. (M) Blood levels of thiamine in CON, CDCA and HB rats. (N) Effects of stigmaterol on expressions of SHP and FGF19 mRNA in HepG2 cell. (O) Plasma concentrations of metformin following oral dose to CON rats, CDCA rats, Stig rats and CDCA + Stig rats. (P) Plasma concentrations of metformin following intravenous dose to CON rats, CDCA rats, Stig rats and CDCA + Stig rats. (Q) Protein expressions of intestinal Oct2, (R) hepatic Oct1 and Oct2 as well as (S) renal Oct2 in CON rats, CDCA rats, Stig rats and CDCA + Stig rats. (T) 6-h renal excretion of thiamine and (U) blood levels of thiamine in CON rats, CDCA rats, Stig rats and CDCA + Stig rats. Data are expressed as mean \pm SD ($n = 6$). * $P < 0.05$, ** $P < 0.01$ vs CON rats or CON cells. # $P < 0.05$ and ### $P < 0.01$ vs CDCA rats or CDCA cells.

shows that BDL significantly decreases plasma metformin exposure following both oral and intravenous dose, accompanied by the increased renal clearance. BDL was reported not affect GFR in rats²⁰, inferring that the increased renal clearance of metformin

mainly comes from the increased renal secretory clearance. The extent of decreases in plasma exposure for oral dose is larger than that for intravenous dose, indicating that the decreases in plasma exposure to metformin following oral dose are attributed to the

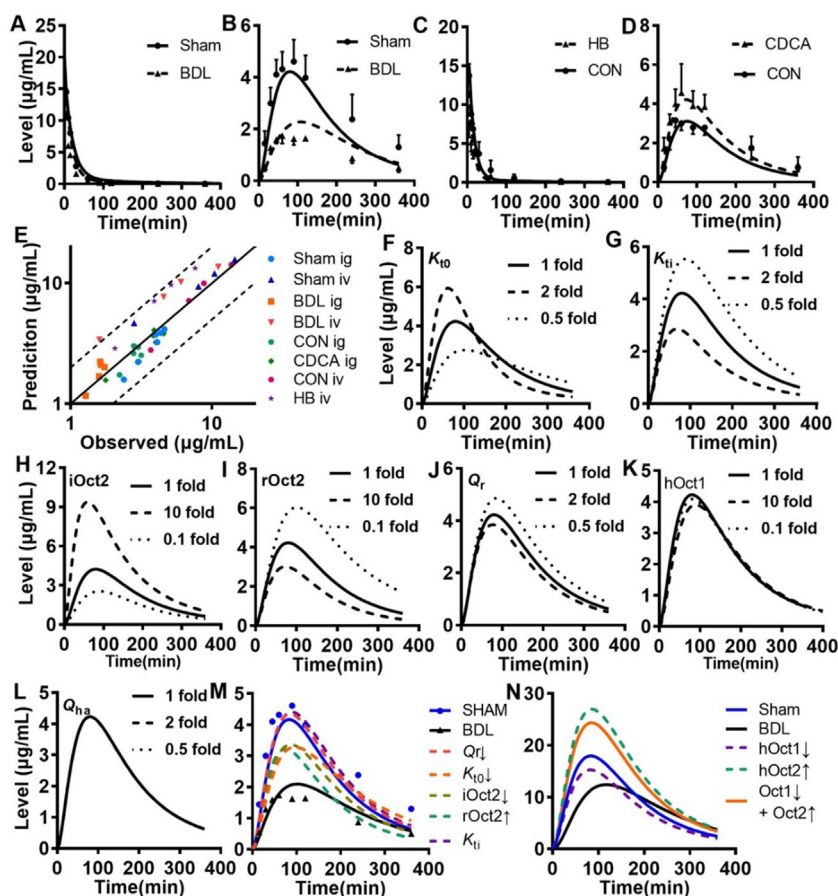


Figure 7 Prediction of metformin pharmacokinetic profiles in rats using semi-PBPK model. (A–D) Predicted (line) and observed (points) plasma concentrations of metformin following intravenous dose (10 mg/kg) (A) and oral dose (40 mg/kg) (B) in BDL and Sham rats, (C) following intravenous dose (10 mg/kg) to bilirubin-treated rats and control rats, following oral dose to control rats and CDCA-treated rats (D). (E) Relationship between the predicted concentrations and the observed concentrations. Solid and dashed lines respectively represent unity and 2-fold errors between observed and predicted data. Individual contributions of alterations in (F) gastric emptying rate (K_{10}), (G) intestinal transport rate (K_{ti}), (H) intestinal Oct2 (iOct2), (I) renal Oct2 (rOct2), (J) renal blood flow (Q_r), (K) hepatic Oct1 (hOct1) and (L) hepatic blood (Q_{ha}) to pharmacokinetics of metformin following oral dose (40 mg/kg) to rats. (M) Individual contribution of alterations in K_{10} , K_{ti} , iOct2, rOct2 and Q_r under BDL to oral pharmacokinetics of metformin and their integrated effects. (N) Predicted levels of metformin in liver of BDL and Sham rats as well as individual contributions of decreased hepatic Oct1 protein and increased Oct2 protein to hepatic levels of metformin and their integration.

integrated effects of the decreases in intestinal absorption and the increases in renal excretion. It is in line with the above deduction that BDL remarkably lowers intestinal absorption of metformin and increases renal uptake of metformin in rats. Protein expressions of corresponding transporters were measured using Western blot. It is contrast to previous reports^{31,32} that protein expressions of intestinal Oct1 are not detected. Several reports have also showed that metformin concentration-time profiles following oral dose in blood of Oct1-knockout mice are comparable to those in wild-type mice^{8,59}. Clinical report also shows that OCT1 genotypes do not affect steady-state pharmacokinetics of metformin in human. These results indicate that intestinal OCT1 seems not to be principally involved in metformin absorption⁶⁰. Protein expressions of Oct2, Oct3 and Thtr2 are detected in small intestine of rats. Moreover, expressions of Oct2, Oct3 and Thtr2 in small intestine are regional. The highest protein expressions of Oct2 and Oct3 occur in duodenum, followed by jejunum and ileum. Expressions of Thtr2 protein is only detected in duodenum. BDL remarkably down-regulates protein expressions of intestinal Oct2 without affecting intestinal Oct3 and intestinal Thtr2, although Oct3^{61,62} and Thtr2¹³

also mediates intestinal absorption of metformin, indicating that decreases in intestinal absorption of metformin by BDL mainly result from downregulation of intestinal Oct2 protein. Neither in line with the above deduction that co-administration of Oct2/3 inhibitor corticosterone rather than Oct1 inhibitor dopamine nor does Oct3 inhibitor estradiol significantly decrease P_{eff} of metformin. The present study also shows that Oct2 protein is mainly expressed at apical membrane of enterocytes, but Oct3 protein is mainly detected at basolateral membrane of enterocytes, partly explaining why estradiol does not affect P_{eff} of metformin.

It is in line with the increased renal excretion and renal uptake of metformin that BDL remarkably upregulates protein expressions of renal Oct2. Significant lower expressions of Oct1 protein but higher expressions of Oct2 protein were also found in liver of BDL rats. Although hepatic uptake of metformin is mainly mediated by Oct1, the contribution of hepatic Oct1 to plasma metformin exposure is minor^{8,48,59}. Furthermore, BDL little affects *in vivo* uptake clearance of metformin and *in vitro* uptake of metformin by hepatocytes, indicating that the inductions of hepatic Oct2 seems to partly attenuate contribution of the decreased

Table 1 Physiological parameters of metformin used in the semi-PBPK model for 250 g rats.

Parameter	Unit	Sham rat	BDL rat
Gastric emptying rate (K_{t0})	min^{-1}	0.0138 ⁴⁴	0.0092 ^a
Duodenum transit time (K_{t1})	min^{-1}	0.799 ⁴⁴	0.682 ^b
Jejunum transit time (K_{t2})	min^{-1}	0.213 ⁴⁴	0.170 ^b
Ileum transit time (K_{t3})	min^{-1}	0.0167 ⁴⁴	0.0133 ^b
Duodenum wall volume (V_{g1})	mL	1.08 ³¹	1.08
Jejunum wall volume (V_{g2})	mL	9.94 ³¹	9.94
Ileum wall volume (V_{g3})	mL	0.32 ³¹	0.32
Portal vein (V_{pv})	mL	0.25 ³¹	0.25
Liver volume	mL	7.0 ^c	16.51 ^c
Liver blood volume (V_{h1})	mL	0.83 ^d	1.95 ^d
Hepatocyte volume (V_{h2})	mL	6.17 ^d	14.56 ^d
Renal volume	mL	1.55 ⁴⁷	1.55 ³⁷
Renal blood volume (V_{r1})	mL	0.23 ^e	0.23 ^e
Tubular volume (V_{r2})	mL	1.32 ^e	1.32 ^e
Duodenum wall blood flow (Q_{g1})	mL/min	1.19 ^f	1.06 ^f
Jejunum wall blood flow (Q_{g2})	mL/min	11.20 ^f	9.97 ^f
Ileum wall blood flow (Q_{g3})	mL/min	0.31 ^f	0.27 ^f
Portal vein blood flow (Q_{pv})	mL/min	12.70 ⁵⁰	11.30 ⁵⁰
Hepatic artery (Q_{ha})	mL/min	2.31 ⁵⁰	13.84 ⁵⁰
Liver blood flow ($Q_h = Q_{ha} + Q_{pv}$)	mL/min	15.01	25.14
Renal blood (Q_R)	mL/min	10.8 ⁵¹	8.4 ⁵¹
Glomerular filtration rate (GFR)	mL/min	2.46 ⁴¹	1.81 ⁴¹
Duodenum radius ($r1$)	cm	0.2 ³¹	0.2
Jejunum radius ($r2$)	cm	0.2 ³¹	0.2
Ileum radius ($r3$)	cm	0.2 ³¹	0.2
Physiological scaling factor (PBSF _{hepatocytes})	$\times 10^6$ cells/g liver	128 ⁵²	128
CL _{int,Oct1,liver}	$\mu\text{L}/\text{min}/10^6$ cells	1.15 ^g	0.52 ^h
CL _{int,Oct2,liver}	$\mu\text{L}/\text{min}/10^6$ cells	0.65 ^g	2.60 ^h
CL _{int,pas,liver}	$\mu\text{L}/\text{min}/10^6$ cell	1.9 ⁵³	1.9
Empirical scaling factor (RAF _{liver})	/	1	1
CL _{non-renal}	mL/min	0.77 ^e	0.77
CL _{int,renal,Mate}	mL/min	6.87 ^h	6.87
PBSF _{kidney}	mg/g kidney	15 ⁱ	15
RAF _{renal,Mate}	/	3 ⁴⁸	3
$V_{\text{max,renal,Oct2}}$	pmol/mg protein/min	1446 ⁵⁶	7042.1 ^l
$K_{\text{m,renal,Oct2}}$	mmol/L	0.63 ⁵⁶	0.63
RAF _{renal,Oct2}	/	46 ^j	46 ^j
$P_{\text{eff,Oct2,duodenum}}$	cm/min	0.00165 ^e	0.000617 ^k
$P_{\text{eff,non-Oct2,duodenum}}$	cm/min	0.00172	0.00172
$P_{\text{eff,Oct2,jejunum}}$	cm/min	0.00083 ^l	0.000365 ^k
$P_{\text{eff,non-Oct2,jejunum}}$	cm/min	0.00172	0.00172
$P_{\text{eff,Oct2,ileum}}$	cm/min	0.00055 ^l	0.00396 ^k
$P_{\text{eff,non-Oct2,ileum}}$	cm/min	0.00172	0.00172
k_{12}	min^{-1}	0.0130 ^j	0.0130
k_{21}	min^{-1}	0.0082 ^j	0.0082
V_1	mL	102.99 ^j	102.99
$K_{h/p}$	/	1.6 ⁴⁸	1.6
$K_{k/p}$	/	1.49 ⁴⁸	1.49
$K_{g/k}$	/	1.5 ⁴⁸	1.5
f_u	/	1.0 ⁴⁸	1.0
R_b	/	1.0 ⁴⁸	1.0

^aCorrected by the increased fraction for prolongation of gastro emptying rate⁴⁵.

^bCorrected by the increased fraction for prolongation of intestinal transit time⁴⁶.

^cMeasurement in the study.

^dHepatic blood volume is assumed to be 11.2%³¹ of hepatic volume.

^eRenal blood volume is assumed to be 12% of renal volume⁴⁸.

^fBlood flow in duodenum wall, jejunum wall and ileum wall account for 9.5%, 88.1% and 2.4% of portal blood flow, respectively⁴⁹.

^gEstimated from data⁵³ and cellular protein content was assumed to be 0.25 mg/10⁶ cells⁵⁴.

^hEstimated from human data³⁸ using equation $(0.25/70)^{0.6755}$.

ⁱAssumed that cellular protein content is 0.25 mg protein/10⁶ cells and numbers of proximal tubule cell are 60×10^6 cells/g kidney⁵⁴.

^jEstimated from original data.

^kEstimated using Sham rats \times relative expressions of targeted protein.

^lEstimated from values of duodenum \times relative expressions of Oct2 protein compared with duodenum, in which expressions of Oct2 protein in jejunum and ileum were measured to be 0.50 and 0.33 of that in duodenum, respectively.

hepatic Oct1. Further study shows that in Sham rats, Oct2/3 inhibitor corticosterone and Oct1 inhibitor dopamine possess similar inhibitory on uptake of metformin by hepatocytes, but in BDL rats, inhibitory effect of corticosterone is remarkably enhanced and inhibitory effect of dopamine is obviously weakened, supporting partly above deduction. Oct2 (not Oct3) protein is also detected in rat liver. In line, co-administration of corticosterone remarkably *in vitro* and *in vivo* uptake clearances of metformin in liver of normal rats, demonstrating that hepatic Oct2 is also involved in hepatic uptake of metformin.

It is consistent with our data that BDL significantly upregulates expressions of renal Oct2 expressions²⁰ and lowers expressions of hepatic Oct1 in rats⁵⁸. However, there are several opposite reports^{19,24,63}. For example, ethynylestradiol-induced cholestiasis significantly lowers expressions of renal Oct2 and hepatic Oct1 protein¹⁹. Significant downregulation of renal Oct2 and Mate1 protein expressions is also detected in liver failure rats induced by ischemia–reperfusion^{24,64}. These discrepancies may result from liver failure induced by different mechanisms.

Next, we investigated the underlying mechanism that BDL differently regulates protein expressions of OCTs in intestine, liver and kidney using Caco-2 cells, HK-2 cells and HepG2 cells. Liver injury is often accompanied by imbalance of internal environment, such as increased inflammatory mediators^{56,57}, imbalance of bile salt homeostasis^{3,65,66} and increased bilirubin^{23,67}. The present study also shows that BDL significantly decreases levels of bile salts in intestinal content and increases levels of plasma bilirubin of rats. Therefore, we investigated whether alterations in levels of 5 bile salts (CDCA, HDCA, CA, DCA, and GCA) and bilirubin are factors that BDL differently regulates protein expressions of OCTs in intestine, liver and kidney. The results show that both CDCA and bilirubin obviously increase the expressions of OCT2 protein in both Caco-2 and HK-2 cells while decrease expressions of OCT1 protein in HepG2 cells. Similarly, CDCA was reported to induce expressions of OCT2 protein in human proximal renal tubular cells⁶⁸. Moreover, BDL significantly decreases content of intestinal CDCA and increases levels of bilirubin in liver and kidney, but levels of intestinal bilirubin and levels of CDCA in liver and kidney of BDL rats are unaltered. These results indicate that downregulation of intestinal Oct2 in BDL rats is mainly attributed to the decreased levels of intestinal CDCA and that the altered expressions of Oct proteins in liver and kidney of BDL rats are mainly attributed to the increased levels of bilirubin, which are confirmed using CDCA-treated rats and bilirubin-treated rats.

CDCA is natural ligand of FXR³⁴. Both bilirubin and CDCA were reported to induce expressions of beta defensin-1 *via* activating FXR³⁵. We designed a series of experiments to investigate whether CDCA or bilirubin upregulates OCT2 and downregulates OCT1 *via* activating FXR. Data from HK-2 cells demonstrate that FXR agonists (CDCA, bilirubin and GW4064) induce and FXR antagonist MCA inhibits mRNA expressions of SHP, a targeted gene of FXR⁴³, confirming that FXR is activated and inhibited. It is consistent with our expectations that CDCA, bilirubin and GW4064 increase expressions of OCT2 protein in both Caco-2 and HK-2 cells, and downregulate expressions of OCT1 in HepG2 cells, all of which are reversed by both FXR inhibitor MCA and FXR siRNA. Moreover, knockdown of FXR itself inhibits expressions of OCT2 protein in Caco-2 and HK-2 cells and upregulates expressions of OCT1 protein in HepG2 cells. It is in line with our report that CDCA and GW4064 were reported to suppress expressions of hepatic OCT1 protein *via* inducing

FXR⁴⁹. Both increased expressions of hepatic and renal Fxr protein and decreased expression of intestinal Fxr protein in BDL rats also support involvement of Fxr in regulation of Octs. OCT2 protein is not detected in HepG2 cells. Primarily cultured rat hepatocytes were further selected to investigate mechanisms that BDL oppositely regulates expressions of hepatic Oct1 and Oct2 protein in rats. The results show that CDCA, bilirubin and GW4064 inhibit expressions of hepatic Oct1 protein but increase expressions of hepatic Oct2 protein, all of which are almost abolished by both MCA and Fxr siRNA. Roles of FXR/Fxr in regulations of OCTs expression have been demonstrated^{69–71}. Knockout Fxr was reported to reduce levels of Oct2 mRNA in renal of mice⁷⁰. Cholic acid (Fxr agonist) feeding may decrease expressions of Oct1 mRNA in liver of wild-type mice but not in Fxr^{-/-} mice⁷⁰. The present study also shows that Fxr antagonist stigmasterol also decreases expressions of intestinal Oct2 protein and attenuates the increased expressions of intestinal Oct2 protein by CDCA. BDL significantly decreases levels of intestinal CDCA and increase levels of bilirubin in liver and kidney of rats, accompanied by decreases in intestinal Fxr protein and increases in hepatic and renal Fxr. Bilirubin and CDCA are natural agonists of FXR/Fxr^{34,35}. Data from HK-2 cells show that in addition to activation of FXR, CDCA and bilirubin also induce expressions of FXR protein, which are similar to findings in rodent hepatic and intestinal cells⁶⁹ as well as HepG2 cells⁷². All these results indicate that BDL affects FXR signaling pathway *via* both induction of FXR/Fxr protein and activation of FXR/Fxr by CDCA and bilirubin. These results give a conclusion that CDCA and bilirubin differently regulate protein expressions of OCTs/Octs through activating FXR/Fxr pathway.

Roles of CDCA and bilirubin in expressions of Octs were confirmed using both CDCA-treated rats and bilirubin-treated rats. It is consistent with our expectation that treatment with oral CDCA significantly induces expressions of intestinal Oct2 protein and increases plasma exposure to metformin following oral dose without affecting expressions of renal Oct2, hepatic Oct1 and Oct2 protein. Treatment with bilirubin induces expressions of renal and hepatic Oct2 protein but inhibits expressions of hepatic Oct1 protein, accompanied by significant decreases in plasma metformin exposure following intravenous dose. A recent study shows that long treatment with metformin impairs activation of intestinal Fxr in mice⁷³. But, data from HepG2 cells demonstrate that metformin (100 $\mu\text{mol/L}$) does not activate FXR or reverse FXR activation by CDCA (Fig. S4). These results infer that interaction of metformin and FXR needs further investigation.

A semi-PBPK characterizing alterations in protein expressions of intestinal, hepatic and renal Octs has been successfully developed to simulate pharmacokinetics of metformin in experimental rats. Individual contributions of several factors to metformin pharmacokinetics following oral dose are intestinal Oct2>renal Oct2>intestinal transit rate > gastric emptying rate > renal blood flow. Contributions of hepatic Oct1 and hepatic blood flow are minor. Simulation analysis shows that decreases in oral plasma exposure of metformin in BDL rats are mainly attributed to integrated effects of decreased gastric emptying rate, decreased intestinal transit rate, decreased expressions of intestinal Oct2 protein, decreased renal blood flow and increased expressions of renal Oct2 protein. The decrease in plasma exposure of metformin is in line with impairment of metformin hypoglycemic effects, indicating dosage of metformin under liver failure should be adjusted, which needs further clinical investigations. Clinical report also has showed

that urinary excretion of cimetidine in liver cirrhosis patients are significantly increased, accompanied by slight increase in renal clearance of cimetidine⁷⁴. Compared with peptic ulcer patients, patients with liver cirrhosis also characterize lower AUC of cimetidine following intravenous and oral dose of cimetidine⁷⁵. Cimetidine is also substrate of OCT2, indicating that decreased AUC of cimetidine under liver cirrhosis results from both the decreased intestinal absorption of cimetidine due to the down-regulated expressions of intestinal OCTs and the increased renal excretion of cimetidine due to increased expressions of renal OCT2.

Consistent with our report that clinical trial has also shown that patients with liver failure have lower thiamine^{14–20,76,77}, characterizing thiamine deficiency. Transport of thiamine is also mediated by OCT1/2, THTR1/2 and MATEs^{2,78}, showing different affinity and capacity. THTR1 and THTR2 show higher affinity than OCT1 and OCT2, but transport capacities of THTR1 and THTR2 are less than those of OCT1 and OCT2^{78–80}, also showing importance of OCT1 and OCT2 in thiamine transport. BDL significantly lowers intestinal absorption of thiamine, which is in accordance with downregulation of intestinal Oct2 expressions. Co-administration of Oct2/3 inhibitor corticosterone significantly inhibits intestinal absorption of thiamine, further demonstrating roles of intestinal Oct2 in intestinal absorption of thiamine. The increased renal excretion of thiamine in BDL rats is also in agreement with the increased upregulation of renal Oct2 protein expressions. Furthermore, CDCA treatment induces expressions of intestinal Oct2 protein and enhances intestinal absorption of thiamine, leading to increases in blood thiamine levels. On the contrast, bilirubin treatment upregulates expressions of renal Oct2 protein and increases renal excretion of thiamine, accompanied by the lower blood thiamine. These results indicate that thiamine deficiency by liver failure is partly attributed to both downregulation of intestinal OCT2 and upregulation of renal OCT2. OCT2, along with OCTN2, also mediates transport of carnitine and its derivatives (such as acylcarnitine), in common regulating carnitine homeostasis. Carnitine in humans comes from food intake or biosynthesized in the liver and kidneys, stored in skeletal muscle and excreted mainly in urine⁸¹. Induction of renal Oct2 and downregulation of intestinal Oct2 by liver failure may partly explain the clinical findings that patients with abnormal liver tests show lower plasma carnitine levels^{82–84} and increased urinary excretion of both free and acylcarnitine⁸¹. The study also has some limitations. For example, BDL decreases plasma exposure of metformin and attenuates hypoglycemic effects of metformin in rats, but whether extents of alterations in expressions of Oct2 in rats are similar to those in human needs further investigation in clinical trials due to existence of species differences in expressions of OCTs and their regulations.

In conclusion, BDL remarkably downregulates expressions of intestinal Oct2 and hepatic Oct1 protein while upregulates expressions of renal and hepatic Oct2 protein in rats, finally, decreasing plasma exposure and impairing hypoglycemic effects of metformin. Alterations in metformin pharmacokinetics can be simulated using a semi-PBPK model.

Acknowledgments

This work was supported by the National Natural Science Foundation of China (Nos. 82173884, 81872930, 82073922 and 81872833), the “Double First-Class” university project (No. CPU2018GY22, China).

Author contributions

Li Liu, Xiaodong Liu, Shijin Hong contributed to the conception of the study; Shijin Hong, Shuai Li, Xiaoyan Meng, Ping Li and Xun Wang performed the experiment; Shijin Hong and Shuai Li performed the data analyses and wrote the manuscript; Xiaoyan Meng and Mengxiang Su helped perform the analysis with constructive discussions.

Conflicts of interest

The authors declare no competing interests.

Appendix A. Supporting information

Supporting data to this article can be found online at <https://doi.org/10.1016/j.apsb.2022.06.010>.

References

- Liu X. SLC family transporters. *Adv Exp Med Biol* 2019;**1141**: 101–202.
- Koepsell H. Organic cation transporters in health and disease. *Pharmacol Rev* 2020;**72**:253–319.
- Koepsell H, Lips K, Volk C. Polyspecific organic cation transporters: structure, function, physiological roles, and biopharmaceutical implications. *Pharm Res (N Y)* 2007;**24**:1227–51.
- Vollmar J, Kim YO, Marquardt JU, Becker D, Galle PR, Schuppan D, et al. Deletion of organic cation transporter Oct3 promotes hepatic fibrosis via upregulation of TGF β . *Am J Physiol Gastrointest Liver Physiol* 2019;**317**:G195–202.
- Gai Z, Visentin M, Hiller C, Krajnc E, Li T, Zhen J, et al. Organic cation transporter 2 overexpression may confer an increased risk of gentamicin-induced nephrotoxicity. *Antimicrob Agents Chemother* 2016;**60**:5573–80.
- Ciarimboli G, Deuster D, Knief A, Sperling M, Holtkamp M, Edemir B, et al. Organic cation transporter 2 mediates cisplatin-induced oto- and nephrotoxicity and is a target for protective interventions. *Am J Pathol* 2010;**176**:1169–80.
- Lautem A, Heise M, Gräsel A, Hoppe-Lotichius M, Weiler N, Foltys D, et al. Downregulation of organic cation transporter 1 (SLC22A1) is associated with tumor progression and reduced patient survival in human cholangiocellular carcinoma. *Int J Oncol* 2013;**42**:1297–304.
- Shu Y, Sheardown SA, Brown C, Owen RP, Zhang S, Castro RA, et al. Effect of genetic variation in the organic cation transporter 1 (OCT1) on metformin action. *J Clin Invest* 2007;**117**:1422–31.
- Reséndiz-Abarca CA, Flores-Alfaro E, Suárez-Sánchez F, Cruz M, Valladares-Salgado A, Del Carmen Alarcón-Romero L, et al. Altered glycemic control associated with polymorphisms in the SLC22A1 (OCT1) gene in a Mexican population with type 2 diabetes mellitus treated with metformin: a cohort study. *J Clin Pharmacol* 2019;**59**: 1384–90.
- Polegato BF, Pereira AG, Azevedo PS, Costa NA, Zornoff LAM, Paiva SAR, et al. Role of thiamin in health and disease. *Nutr Clin Pract* 2019;**34**:558–64.
- Zhao R, Goldman ID. Folate and thiamine transporters mediated by facilitative carriers (SLC19A1-3 and SLC46A1) and folate receptors. *Mol Aspects Med* 2013;**34**:373–85.
- Reidling JC, Lambrecht N, Kassir M, Said HM. Impaired intestinal vitamin B1 (thiamin) uptake in thiamin transporter-2-deficient mice. *Gastroenterology* 2010;**138**:1802–9.
- Liang X, Chien HC, Yee SW, Giacomini MM, Chen EC, Piao M, et al. Metformin is a substrate and inhibitor of the human thiamine transporter, THTR-2 (SLC19A3). *Mol Pharm* 2015;**12**:4301–10.

14. Butterworth RF. Thiamine deficiency-related brain dysfunction in chronic liver failure. *Metab Brain Dis* 2009;**24**:189–96.
15. Rossouw JE, Labadarios D, Krasner N, Davis M, Williams R. Red blood cell transketolase activity and the effect of thiamine supplementation in patients with chronic liver disease. *Scand J Gastroenterol* 1978;**13**:133–8.
16. Labadarios D, Rossouw JE, McConnell JB, Davis M, Williams R. Thiamine deficiency in fulminant hepatic failure and effects of supplementation. *Int J Vitam Nutr Res* 1977;**47**:17–22.
17. Gupta RK, Yadav SK, Saraswat VA, Rangan M, Srivastava A, Yadav A, et al. Thiamine deficiency related microstructural brain changes in acute and acute-on-chronic liver failure of non-alcoholic etiology. *Clin Nutr* 2012;**31**:422–8.
18. Srivastava A, Yadav SK, Borkar VV, Yadav A, Yachha SK, Thomas MA, et al. Serial evaluation of children with ALF with advanced MRI, serum proinflammatory cytokines, thiamine, and cognition assessment. *J Pediatr Gastroenterol Nutr* 2012;**55**:580–6.
19. Jin HE, Hong SS, Choi MK, Maeng HJ, Kim DD, Chung SJ, et al. Reduced antidiabetic effect of metformin and down-regulation of hepatic Oct1 in rats with ethynylestradiol-induced cholestasis. *Pharm Res (N Y)* 2009;**26**:549–59.
20. Kurata T, Muraki Y, Mizutani H, Iwamoto T, Okuda M. Elevated systemic elimination of cimetidine in rats with acute biliary obstruction: the role of renal organic cation transporter OCT2. *Drug Metab Pharmacokinet* 2010;**25**:328–34.
21. Li Y, Zhang J, Xu P, Sun B, Zhong Z, Liu C, et al. Acute liver failure impairs function and expression of breast cancer-resistant protein (BCRP) at rat blood–brain barrier partly via ammonia-ROS-ERK1/2 activation. *J Neurochem* 2016;**138**:282–94.
22. Liu L, Miao M, Chen Y, Wang Z, Sun B, Liu X. Altered function and expression of ABC transporters at the blood–brain barrier and increased brain distribution of phenobarbital in acute liver failure mice. *Front Pharmacol* 2018;**9**:190.
23. Xu P, Ling ZL, Zhang J, Li Y, Shu N, Zhong ZY, et al. Unconjugated bilirubin elevation impairs the function and expression of breast cancer resistance protein (BCRP) at the blood–brain barrier in bile duct-ligated rats. *Acta Pharmacol Sin* 2016;**37**:1129–40.
24. Ikemura K, Nakagawa E, Kurata T, Iwamoto T, Okuda M. Altered pharmacokinetics of cimetidine caused by down-regulation of renal rat organic cation transporter 2 (rOCT2) after liver ischemia–reperfusion injury. *Drug Metab Pharmacokinet* 2013;**28**:504–9.
25. Patidar KR, Bajaj JS. Covert and overt hepatic encephalopathy: diagnosis and management. *Clin Gastroenterol Hepatol* 2015;**13**:2048–61.
26. Graham GG, Punt J, Arora M, Day RO, Doogue MP, Duong JK, et al. Clinical pharmacokinetics of metformin. *Clin Pharmacokinet* 2011;**50**:81–98.
27. Chen Y, Li H, Xu J, et al. Determination of metformin in diabetic rat plasma by an improved ion-pair high-performance liquid chromatography: application to a pharmacokinetic study. *J Chin Pharm Sci* 2012;**21**:211–8.
28. Komazawa H, Yamaguchi H, Hidaka K, Ogura J, Kobayashi M, Iseki K. Renal uptake of substrates for organic anion transporters Oat1 and Oat3 and organic cation transporters Oct1 and Oct2 is altered in rats with adenine-induced chronic renal failure. *J Pharm Sci* 2013;**102**:1086–94.
29. Yang T, Wang S, Liu P, Xu J, Liu X, L L. Influence on compatibility of glycyrrhiza uralensis and *Laminaria japonica* on liver and kidney functions and serum indexes in rats. *Chin Tradit Herb Drugs* 2018;**49**:1860–5.
30. Xie F, Cheng Z, Li S, Liu X, Guo X, Yu P, et al. Pharmacokinetic study of benfotiamine and the bioavailability assessment compared to thiamine hydrochloride. *J Clin Pharmacol* 2014;**54**:688–95.
31. Wang Z, Yang H, Xu J, Zhao K, Chen Y, Liang L, et al. Prediction of atorvastatin pharmacokinetics in high-fat diet and low-dose streptozotocin-induced diabetic rats using a semiphysiologically based pharmacokinetic model involving both enzymes and transporters. *Drug Metab Dispos* 2019;**47**:1066–79.
32. Sainio EL, Lehtola T, Roininen P. Steroids. Radioimmunoassay of total and free corticosterone in rat plasma: measurement of the effect of different doses of corticosterone. *Steroids* 1988;**51**:609–22.
33. Liang LM, Zhou JJ, Xu F, Liu PH, Qin L, Liu L, et al. Diabetes downregulates peptide transporter 1 in the rat jejunum: possible involvement of cholate-induced FXR activation. *Acta Pharmacol Sin* 2020;**41**:1465–75.
34. Ali AH, Carey EJ, Lindor KD. Recent advances in the development of farnesoid X receptor agonists. *Ann Transl Med* 2015;**3**:5.
35. Klag T, Thomas M, Ehmann D, Courth L, Mailander-Sanchez D, Weiss TS, et al. beta-Defensin 1 is prominent in the liver and induced during cholestasis by bilirubin and bile acids via farnesoid X receptor and constitutive androstane receptor. *Front Immunol* 2018;**9**:1735.
36. Gonzalez FJ, Jiang C, Patterson AD. An intestinal microbiota-farnesoid X receptor axis modulates metabolic disease. *Gastroenterology* 2016;**151**:845–59.
37. Carter BA, Taylor OA, Prendergast DR, Zimmerman TL, Von Furstenberg R, Moore DD, et al. Stigmasterol, a soy lipid-derived phytosterol, is an antagonist of the bile acid nuclear receptor FXR. *Pediatr Res* 2007;**62**:301–6.
38. El Kasmi KC, Anderson AL, Devereaux MW, Vue PM, Zhang W, Setchell KD, et al. Phytosterols promote liver injury and Kupffer cell activation in parenteral nutrition-associated liver disease. *Sci Transl Med* 2013;**5**:206–37.
39. Ahmad Khan M, Sarwar AHMG, Rahat R, Ahmed RS, Umar S. Stigmasterol protects rats from collagen induced arthritis by inhibiting proinflammatory cytokines. *Int Immunopharmacol* 2020;**85**:106–642.
40. Han TK, Everett RS, Proctor WR, Ng CM, Costales CL, Brouwer KL, et al. Organic cation transporter 1 (OCT1/mOct1) is localized in the apical membrane of Caco-2 cell monolayers and enterocytes. *Mol Pharmacol* 2013;**84**:182–9.
41. Jin S, Lee S, Jeon JH, Kim H, Choi MK, Song IS. Enhanced intestinal permeability and plasma concentration of metformin in rats by the repeated administration of red ginseng extract. *Pharmaceutics* 2019;**11**:189.
42. Saborowski M, Kullak-Ublick GA, Eloranta JJ. The human organic cation transporter-1 gene is transactivated by hepatocyte nuclear factor-4alpha. *J Pharmacol Exp Ther* 2006;**317**:778–85.
43. Manley S, Ding W. Role of farnesoid X receptor and bile acids in alcoholic liver disease. *Acta Pharm Sin B* 2015;**5**:158–67.
44. Kadono K, Yokoe J, Ogawara K, Higaki K, Kimura T. Analysis and prediction of absorption behavior for theophylline orally administered as powders based on gastrointestinal-transit-absorption (GitA) model. *Drug Metab Pharmacokinet* 2002;**17**:307–15.
45. Ishizu H, Shiomi S, Kawamura E, Iwata Y, Nishiguchi S, Kawabe J, et al. Gastric emptying in patients with chronic liver diseases. *Ann Nucl Med* 2002;**16**:177–82.
46. Liu M, Zheng SJ, Xu W, Zhang J, Chen Y, Duan Z. Changing interdigestive migrating motor complex in rats under acute liver injury. *BioMed Res Int* 2014;**2014**:634281.
47. Larson M, Sjoquist M, Wolgast M. Renal interstitial volume of the rat kidney. *Acta Physiol Scand* 1984;**120**:297–304.
48. Yang Y, Zhang Z, Li P, Kong W, Liu X, Liu L. A whole-body physiologically based pharmacokinetic model characterizing interplay of OCTs and MATEs in intestine, liver and kidney to predict drug–drug interactions of metformin with perpetrators. *Pharmaceutics* 2021;**13**:698.
49. Zhang J, Xie Q, Kong W, Wang Z, Wang S, Zhao K, et al. Short-chain fatty acids oppositely altered expressions and functions of intestinal cytochrome P4503A and P-glycoprotein and affected pharmacokinetics of verapamil following oral administration to rats. *J Pharm Pharmacol* 2020;**72**:448–60.
50. Chouhan MD, Taylor SA, Bainbridge A, Walker-Samuel S, Davies N, Halligan S, et al. Haemodynamic changes in cirrhosis following terlipressin and induction of sepsis—a preclinical study using caval subtraction phase-contrast and cardiac MRI. *Eur Radiol* 2021;**31**:2518–28.
51. Maoka T, Kawata T, Koike T, Mochizuki T, Schnermann J, Hashimoto S. Defective renal autoregulation in the chronic bile duct ligation model of liver failure. *Clin Exp Nephrol* 2018;**22**:1052–60.

52. Ring BJ, Chien JY, Adkison KK, Jones HM, Rowland M, Jones RD, et al. PhRMA CPDC initiative on predictive models of human pharmacokinetics, part 3: comparative assessment of prediction methods of human clearance. *J Pharm Sci* 2011;**100**:4090–110.
53. Umehara KI, Iwatsubo T, Noguchi K, Kamimura H. Functional involvement of organic cation transporter1 (OCT1/Oct1) in the hepatic uptake of organic cations in humans and rats. *Xenobiotica* 2007;**37**:818–31.
54. Mathialagan S, Piotrowski MA, Tess DA, Feng B, Litchfield J, Varma MV. Quantitative prediction of human renal clearance and drug–drug interactions of organic anion transporter substrates using *in vitro* transport data: a relative activity factor approach. *Drug Metab Dispos* 2017;**45**:409–17.
55. Kong WM, Sun BB, Wang ZJ, Zheng XK, Zhao KJ, Chen Y, et al. Physiologically based pharmacokinetic-pharmacodynamic modeling for prediction of vonoprazan pharmacokinetics and its inhibition on gastric acid secretion following intravenous/oral administration to rats, dogs and humans. *Acta Pharmacol Sin* 2020;**41**:852–65.
56. Kimura N, Masuda S, Tanihara Y, Ueo H, Okuda M, Katsura T, et al. Metformin is a superior substrate for renal organic cation transporter OCT2 rather than hepatic OCT1. *Drug Metab Pharmacokinet* 2005;**20**:379–86.
57. Guest EJ, Aarons L, Houston JB, Rostami-Hodjegan A, Galetin A. Critique of the two-fold measure of prediction success for ratios: application for the assessment of drug–drug interactions. *Drug Metab Dispos* 2011;**39**:170–3.
58. Denk GU, Soroka CJ, Mennone A, Koepsell H, Beuers U, Boyer JL. Down-regulation of the organic cation transporter 1 of rat liver in obstructive cholestasis. *Hepatology* 2004;**39**:1382–9.
59. Shu Y, Brown C, Castro RA, Shi RJ, Lin ET, Owen RP, et al. Effect of genetic variation in the organic cation transporter 1, OCT1, on metformin pharmacokinetics. *Clin Pharmacol Ther* 2008;**83**:273–80.
60. Wenzel C, Drozdik M, Oswald S. Organic cation transporter 1 an intestinal uptake transporter: fact or fiction?. *Front Pharmacol* 2021;**12**:648388.
61. Chen EC, Liang X, Yee SW, Geier EG, Stocker SL, Chen L, et al. Targeted disruption of organic cation transporter 3 attenuates the pharmacologic response to metformin. *Mol Pharmacol* 2015;**88**:75–83.
62. Shirasaka Y, Lee N, Zha W, Wagner D, Wang J. Involvement of organic cation transporter 3 (OCT3/Slc22a3) in the bioavailability and pharmacokinetics of antidiabetic metformin in mice. *Drug Metab Pharmacokinet* 2016;**31**:385–8.
63. Matsuzaki T, Morisaki T, Sugimoto W, Yokoo K, Sato D, Nonoguchi H, et al. Altered pharmacokinetics of cationic drugs caused by down-regulation of renal rat organic cation transporter 2 (Slc22a2) and rat multidrug and toxin extrusion 1 (Slc47a1) in ischemia/reperfusion-induced acute kidney injury. *Drug Metab Dispos* 2008;**36**:649–54.
64. Adebayo D, Morabito V, Davenport A, Jalan R. Renal dysfunction in cirrhosis is not just a vasomotor nephropathy. *Kidney Int* 2015;**87**:509–15.
65. Fukui H. Gut-liver axis in liver cirrhosis: how to manage leaky gut and endotoxemia. *World J Hepatol* 2015;**7**:425–42.
66. Bajaj JS, Kakiyama G, Zhao D, Takei H, Fagan A, Hylemon P, et al. Continued alcohol misuse in human cirrhosis is associated with an impaired gut-liver axis. *Alcohol Clin Exp Res* 2017;**41**:1857–65.
67. van Slambrouck CM, Salem F, Meehan SM, Chang A. Bile cast nephropathy is a common pathologic finding for kidney injury associated with severe liver dysfunction. *Kidney Int* 2013;**84**:192–7.
68. Israeli BA, Bogin E. Biochemical changes in liver, kidney and blood associated with common bile duct ligation. *Clin Chim Acta* 1986;**160**:211–21.
69. Wongwan T, Chatsudhipong V, Soodvilai S. Farnesoid X receptor activation stimulates organic cations transport in human renal proximal tubular cells. *Int J Mol Sci* 2020;**21**:6078.
70. Hyrsova L, Smutny T, Trejtnar F, Pavek P. Expression of organic cation transporter 1 (OCT1): unique patterns of indirect regulation by nuclear receptors and hepatospecific gene regulation. *Drug Metab Rev* 2016;**48**:139–58.
71. Maeda T, Miyata M, Yotsumoto T, Kobayashi D, Nozawa T, Toyama K, et al. Regulation of drug transporters by the farnesoid X receptor in mice. *Mol Pharm* 2004;**1**:281–9.
72. Martin P, Riley R, Thompson P, Williams D, Back D, Owen A. Effect of prototypical inducers on ligand activated nuclear receptor regulated drug disposition genes in rodent hepatic and intestinal cells. *Acta Pharmacol Sin* 2010;**31**:51–65.
73. Lew JL, Zhao A, Yu J, Huang L, De Pedro N, Peláez F, et al. The farnesoid X receptor controls gene expression in a ligand- and promoter-selective fashion. *J Biol Chem* 2004;**279**:8856–61.
74. Gugler R, Müller-Liebenau B, Somogyi A. Altered disposition and availability of cimetidine in liver cirrhotic patients. *Br J Clin Pharmacol* 1982;**14**:421–30.
75. Sonne J, Poulsen HE, Døssing M, Larsen NE, Andreasen PB. Cimetidine clearance and bioavailability in hepatic cirrhosis. *Clin Pharmacol Ther* 1981;**29**:191–7.
76. Bosoi CR, Rose CF. Elevated cerebral lactate: implications in the pathogenesis of hepatic encephalopathy. *Metab Brain Dis* 2014;**29**:919–25.
77. Ott M, Werneke U. Wernicke's encephalopathy—from basic science to clinical practice. Part 1: understanding the role of thiamine. *Ther Adv Psychopharmacol* 2020;**10**:2045125320978106.
78. Kato K, Mori H, Kito T, Yokochi M, Ito S, Inoue K, et al. Investigation of endogenous compounds for assessing the drug interactions in the urinary excretion involving multidrug and toxin extrusion proteins. *Pharm Res (N Y)* 2014;**31**:136–47.
79. Chen L, Shu Y, Liang X, Chen EC, Yee SW, Zur AA, et al. OCT1 is a high-capacity thiamine transporter that regulates hepatic steatosis and is a target of metformin. *Proc Natl Acad Sci U S A* 2014;**111**:9983–8.
80. Giacomini MMOL/L, Hao J, Liang X, Chandrasekhar J, Twelves J, Whitney JA, et al. Interaction of 2,4-diaminopyrimidine-containing drugs including fedratinib and trimethoprim with thiamine transporters. *Drug Metab Dispos* 2017;**45**:76–85.
81. Tanphaichitr V, Leelahagul P. Carnitine metabolism and human carnitine deficiency. *Nutrition* 1993;**9**:246–54.
82. Bowyer BA, Miles JM, Haymond MW, Fleming CR. L-Carnitine therapy in home parenteral nutrition patients with abnormal liver tests and low plasma carnitine concentrations. *Gastroenterology* 1988;**94**:434–8.
83. Matsuda I, Ohtani Y. Carnitine status in reye and reye-like syndromes. *Pediatr Neurol* 1986;**2**:90–4.
84. Nowaczyk MJ, Whelan D, Hill RE, Clarke JT, Pollitt RJ. Long-chain hydroxydicarboxylic aciduria, carnitine depletion and acetaminophen exposure. *J Inher Metab Dis* 2000;**23**:188–9.